Hepatocyte-specific deletion of HIF2α prevents NASH-related liver carcinogenesis by decreasing cancer cell proliferation

Hepatocyte-specific deletion of HIF2α prevents NASH-related liver carcinogenesis by decreasing cancer cell proliferation

Beatrice Foglia, Salvatore Sutti, Stefania Cannito, Chiara Rosso, Marina Maggiora, Riccardo Autelli, Erica Novo, Claudia Bocca, Gianmarco Villano, Naresh Naik Ramavath, Ramy Younes, Ignazia Tusa, Elisabetta Rovida, Patrizia Pontisso, Elisabetta Bugianesi, Emanuele Albano, Maurizio Parola

PII: S2352-345X(21)00216-2
DOI: https://doi.org/10.1016/j.jcmgh.2021.10.002
Reference: JCMGH 905

To appear in: *Cellular and Molecular Gastroenterology and Hepatology*
Accepted Date: 6 October 2021

Please cite this article as: Foglia B, Sutti S, Cannito S, Rosso C, Maggiora M, Autelli R, Novo E, Bocca C, Villano G, Ramavath NN, Younes R, Tusa I, Rovida E, Pontisso P, Bugianesi E, Albano E, Parola M, Hepatocyte-specific deletion of HIF2α prevents NASH-related liver carcinogenesis by decreasing cancer cell proliferation, *Cellular and Molecular Gastroenterology and Hepatology* (2021), doi: https://doi.org/10.1016/j.jcmgh.2021.10.002.

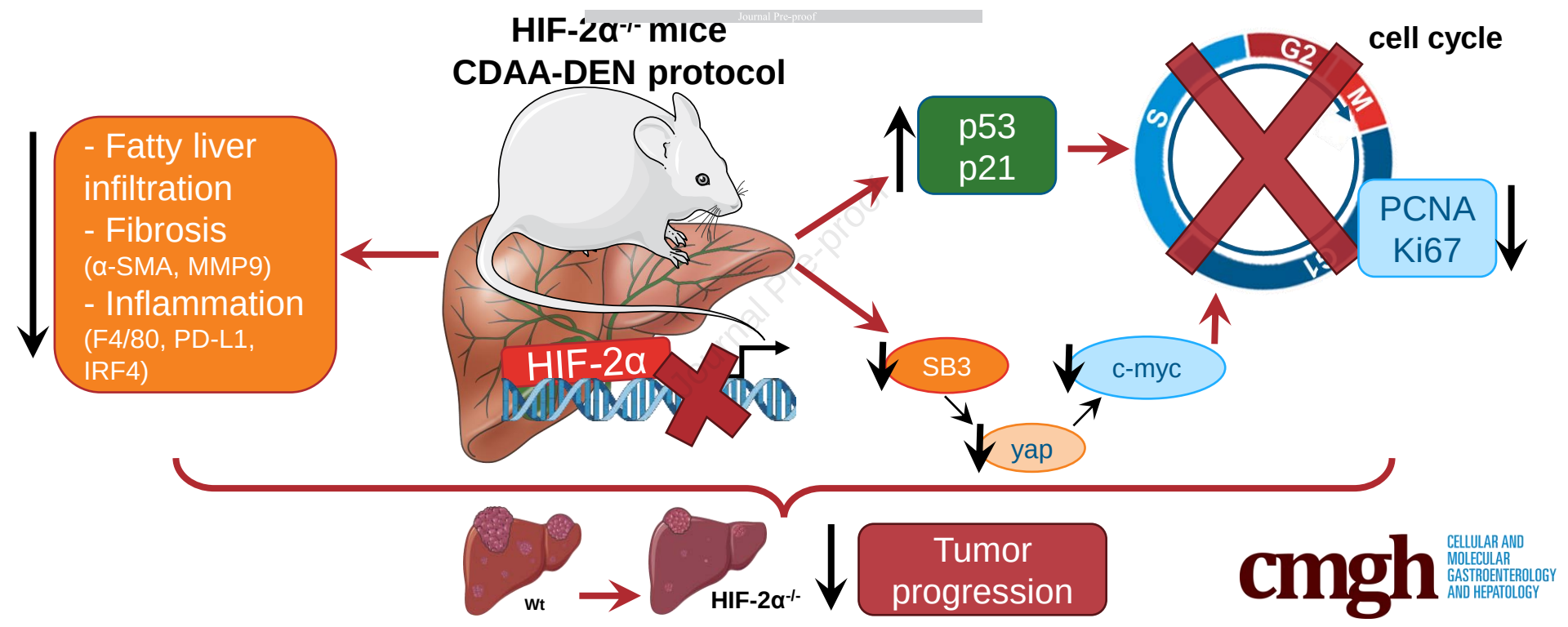

cmgh CELLULAR AND MOLECULAR GASTROENTEROLOGY AND HEPATOLOGY

Hepatocyte-specific deletion of HIF2α prevents NASH-related liver carcinogenesis by decreasing cancer cell proliferation

Short title: HIF2α deletion prevents NASH-related liver carcinogenesis

Beatrice Foglia[1*], Salvatore Sutti[2*], Stefania Cannito[1], Chiara Rosso[3], Marina Maggiora[1], Riccardo Autelli[1], Erica Novo[1], Claudia Bocca[1], Gianmarco Villano[4], Naresh Naik Ramavath[2], Ramy Younes[3], Ignazia Tusa[5], Elisabetta Rovida[5], Patrizia Pontisso[4], Elisabetta Bugianesi[3], Emanuele Albano[2#], Maurizio Parola[1#].

[1]Dept. Clinical and Biological Sciences, Unit of Experimental Medicine and Clinical Pathology, University of Torino, Italy; [2]Dept. Health Sciences and Interdisciplinary Research Centre for Autoimmune Diseases, University Amedeo Avogadro of East Piedmont, Novara, Italy; [3]Dept. Medical Sciences, University of Torino, and Division of Gastroenterology, San Giovanni Hospital, Torino, Italy; [4]Dept. Medicine, University of Padova, Italy; [5]Dept. Experimental and Clinical Biomedical Sciences, Unit of Experimental Oncology and Pathology, University of Florence, Italy.

*These Authors contributed equally to this study

#These Authors contributed equally to this study and shared senior authorship.

Grant support. The research leading to these results has received funding from: i) AIRC under IG 2014 ID. 15274 project – P.I. Parola Maurizio; ii) European Union's Horizon 2020 research and innovation programme under grant agreement No. 634413 for the project EPoS (Elucidating Pathways of Steatohepatitis) (to EB); iii) The CariPLO Foundation (Milan, Italy), grant n. 2011-0470 (to EA and MP); iv) The University of Torino (Torino, Italy), (to EN and MP); v) the University of Padova (Project No. CPDA110795 – PP). The funders had no role in the study design, data collection and analysis, decision to publish, or preparation of the manuscript.

Abbreviations.

HIFs, Hypoxia-inducible factors; ROS, reactive oxygen species; YAP, Yes Associated Protein

Correspondence

Address correspondence to: Maurizio Parola, PhD, Dept. Clinical and Biological Sciences, Unit of Experimental Medicine and Clinical Pathology, University of Torino, Italy - Corso Raffaello 30, 10125 Torino, Italy. Phone: +39-011-6707772. Fax: +39-011-6707753. e-mail: maurizio.parola@unito.it

Conflict of interest

The authors disclose no conflicts.

CRediT Authorship Contributions

Beatrice Foglia (Conceptualization: Supporting; Formal analysis: Equal; Investigation: Equal; Methodology: Lead; Supervision: Equal; Writing – review & editing: Supporting)

Salvatore Sutti (Conceptualization: Supporting; Formal analysis: Equal; Investigation: Equal; Methodology: Lead; Supervision: Equal; Writing – review & editing: Supporting)

Stefania Cannito (Formal analysis: Supporting; Investigation: Supporting; Writing – review & editing: Supporting)

Chiara Rosso (Formal analysis: Supporting; Investigation: Supporting; Writing – review & editing: Supporting)

Marina Maggiora (Formal analysis: Supporting; Investigation: Supporting; Methodology: Supporting)

Riccardo Autelli (Formal analysis: Supporting; Investigation: Supporting; Methodology: Supporting; Writing – review & editing: Supporting)

Erica Novo (Formal analysis: Supporting; Investigation: Supporting)

Claudia Bocca (Formal analysis: Supporting; Investigation: Supporting)

Gianmarco Villano (Formal analysis: Supporting; Investigation: Supporting; Methodology: Supporting)

Naresh Naik Ramavath (Formal analysis: Supporting; Investigation: Supporting)

Ramy Younes (Formal analysis: Supporting; Investigation: Supporting)

Ignazia Tusa (Formal analysis: Supporting; Investigation: Supporting)

Elisabetta Rovida (Formal analysis: Supporting; Investigation: Supporting; Writing – review & editing: Supporting)

Patrizia Pontisso (Conceptualization: Supporting; Writing – original draft: Supporting; Writing – review & editing: Supporting)

Elisabetta Bugianesi (Conceptualization: Supporting; Data curation: Supporting; Formal analysis: Supporting; Funding acquisition: Supporting; Supervision: Supporting; Writing – original draft: Supporting; Writing – review & editing: Supporting)

Emanuele Albano (Conceptualization: Supporting; Data curation: Supporting; Formal analysis: Supporting; Methodology: Supporting; Funding acquisition: Supporting; Supervision: Supporting; Writing – original draft: Supporting; Writing – review & editing: Supporting)

Maurizio Parola (Conceptualization: Lead; Data curation: Lead; Formal analysis: Lead; Funding acquisition: Lead; Investigation: Lead; Methodology: Supporting; Project administration: Lead; Supervision: Lead; Writing – original draft: Lead; Writing – review & editing: Lead)

Word count: 3444 words (for main document text, not including methods, tables/figures, or references)

Synopsis/Summary: 40 words

Hypoxia-inducible factor 2α (HIF2α) is up-regulated in NAFLD progression. Experiments performed in mice carrying hepatocyte-specific deletion of HIF2α provide the first mechanistic evidence, reinforced by analyses on cancer cells and human samples, that HIF2α is critical for NASH-related liver carcinogenesis.

ABSTRACT (max 260 words)

Background & Aims: Hypoxia and HIFs (hypoxia inducible factors) are involved in chronic liver disease progression. We previously showed that hepatocyte HIF-2α activation significantly contributed to NAFLD progression in experimental animals and human patients. In this study we investigated mechanistically, using an appropriate genetic murine model, the involvement of hepatocyte HIF-2α in experimental NASH-related carcinogenesis.

Methods: The role of HIF-2α, was investigated by morphological, cellular and molecular biology approaches in: a) mice carrying hepatocyte-specific deletion of HIF-2α *(HIF-2α$^{-/-}$* mice) undergoing a NASH-related protocol of hepatocarcinogenesis; b) *HepG2* cells stably transfected to overexpress HIF-2α; c) liver specimens from NASH patients with HCC.

Results: Mice carrying hepatocyte specific deletion of HIF-2α (*hHIF-2α$^{-/-}$*) showed a significant decrease in the volume and number of liver tumors as compared to *wild type* littermates. These effects did not involve HIF-1α changes and were associated with a decrease of cell proliferation markers PCNA and Ki67. In both human and rodent NAFLD-related tumors, HIF-2α levels were strictly associated with hepatocyte production of SerpinB3, a mediator previously shown to stimulate liver cancer cell proliferation through Hippo/YAP/c-Myc pathway. Consistently, we observed positive correlations between the transcripts of HIF-2α, YAP and c-Myc in individual HCC tumor masses, while HIF-2α deletion down-modulated c-Myc and YAP expression without affecting ERK1/2, JNK and AKT-dependent signaling. *In vitro* data confirmed that HIF-2α overexpression induced *HepG2* cell proliferation through YAP-mediated mechanisms.

Conclusions: These results indicate that the activation of HIF-2α in hepatocytes has a critical role in liver carcinogenesis during NASH progression suggesting that HIF-2α-blocking agents may serve as putative novel therapeutic tools.

Keywords: HIF-2α; NAFLD; NASH; hepatocellular carcinoma.

Abstract word count: 257

Non-alcoholic fatty liver disease (NAFLD) is emerging as the most common cause of chronic liver disease (CLD) worldwide with a global prevalence of 25% in the general population and even higher among obese individuals and/or patients affected by Type II diabetes mellitus. [1-3] Approximately 20-30% of NAFLD patients can develop non-alcoholic steatohepatitis (NASH), which is characterized by hepatocyte injury and lobular inflammation and can progress to fibrosis, cirrhosis and liver failure [1,2]. NAFLD patients also show a steadily rising trend to develop hepatocellular carcinoma (HCC) [4,5], the most common primary liver cancer (70%–90%), representing the 4th leading cause of cancer mortality worldwide and with a minority of patients surviving at 5 years from diagnosis, despite treatment. Moreover, NAFLD-associated HCC can also arise in non-cirrhotic liver, [4,5] a worrisome issue considering the high prevalence of NAFLD in the general population and the lack of validated therapy for this disease. [1,2]

In recent years, growing evidence has shown that hepatic hypoxia is involved in CLD progression and in HCC development by sustaining angiogenesis, fibrogenesis and possibly inflammatory and autophagy responses. [7-9] HCC is considered as one of the most hypoxic tumor with a reported median oxygen tension lower than 1.0%. [10,11] The cellular response to hypoxia mainly relays on heterodimeric transcriptional HIFs (hypoxia-inducible factors). These factors consist of an oxygen-sensitive α-subunit (HIF-1α or HIF-2α) and a constitutive β-subunit (HIF-1β). [12,13] Although in the liver HIF-1α and HIF-2α can modulate common transcriptional programs, they often up-regulate distinct and non-overlapping responses. [12,13] Studies in HCCs with different etiology and HCC cell lines indicate that HIF-1α activation may contribute to tumor development by stimulating cell proliferation, metabolic changes, angiogenesis, invasion and metastasis. [8,10,11] Furthermore, HIF-1α overexpression associates with a poor prognosis and HCC resistance to therapy. [10,14] Conversely, the contribution of HIF-2α to HCC development is less well characterized in relation to conflicting results concerning its impact on liver carcinogenesis, particularly on cell survival and

proliferation, [15-19] and also as a consequence of using not-mechanistic/genetic *in vivo* experimental approaches. [20] Furthermore, it has been suggested that the knockdown of HIF-1α enhances the expression of HIF-2α and vice-versa. [19] In the setting of NAFLD, it has been shown that HIF-2α, but not HIF-1α, can up-regulate genes involved in fatty acid synthesis/uptake and lipid storage, while it down-regulates those involved in fatty acid catabolism. [21,22] In a previous study we showed that hepatocyte-specific HIF-2α deletion resulted in a significant decrease of fatty liver, parenchymal injury, lobular inflammation in NAFLD and ameliorated the disease progression towards fibrosis. [23] More recently, a study performed on a limited number of NASH patients carrying HCC, has proposed that HIF-2α expression may be increased in NAFLD-related HCC vs HCC of different etiology [20]. In the present study, by employing mice carrying hepatocyte conditional deletion of HIF-2α and additional in vitro approaches, we provide the first mechanistic and unequivocal evidence that HIF-2α plays a critical role in the development of NASH-related carcinogenesis by promoting liver cancer cell proliferation. Finally, we also provide confirming evidence that HIF-2α expression is up-regulated in a high percentage of human patients carrying NASH-related HCC.

Results

Hepatocyte-specific deletion of HIF-2α reduces the development of NAFLD-associated HHCs

In order to mechanistically investigate the role of HIF2α in the development of NAFLD-related primary liver cancer we employed mice carrying a hepatocyte-specific HIF-2α deletion (*hHIF-2α*$^{-/-}$ mice) already used in a previous study that unequivocally outlined the relevant role of HIF2α in either human or murine NAFLD progression. [23] In the present study these mice and related control littermates were submitted to an established murine model of NAFLD-associated hepatocarcinogenesis based on a single injection of diethyl-nitrosamine (DEN) at 2 weeks of age and the subsequent induction of steatohepatitis by the administration of a choline-deficient L-aminoacid-defined (CDAA) diet for 25 weeks (Figure 1A). [24] The mouse HCC arising in *Wt* mice (characterized by nuclear atypia, pleomorphism, and increased mitotic activity, resembling human Edmonson-Steiner G1/G2 grading) showed diffuse parenchymal cell fat accumulation (Figure 1B,C) consistent with the features of the steatohepatitic HCC often detected among NAFLD patients. [25] Although tumor cell morphology was not appreciably modified, hematoxylin/eosin staining showed a reduced fatty infiltration in liver tumors from mice lacking HIF-2α (Figure 1B,C).The analysis of HIF-2α protein levels in individual mouse HCC from *Wt* mice exposed to DEN/CDAA treatment revealed that HIF-2α expression was upregulated in cancer cells as compared to healthy livers of *wild type* mice fed with the CSAA control diet (*Wt CSAA*) (Figure 2A). *hHIF-2α*$^{-/-}$ mice submitted to DEN/CDAA protocol developed mouse HCC with a HIF-2α mRNA and protein content greatly lower than those from *Wt* mice (Figure 2B,C), as expected. Similarly, neoplastic cells showed a reduced expression of HIF-2α-dependent genes such as CXCR4 and EPO (Figure 2D-E). On the other hand, the transcripts and protein levels of HIF-1α as well as the transcripts levels of HIF-1α-related pro-angiogenic factors such as VEGF-A, VEGFR2 and VE-cadherin, were not significantly different between liver tumors from *hHIF-2α*$^{-/-}$ and *Wt* mice (Figure 3A,B,C). Moreover, no significant change was observed concerning protein levels of CD105 (endoglin), a pro-angiogenic factor, between tumors from *hHIF-2α*$^{-/-}$ and *Wt* mice (Figure 3D). These data overall suggest that hepatocyte-specific HIF-2α deletion does not result in major changes in angiogenic response. Interestingly, both the number and the size of mouse HCC that developed in *hHIF-2α*$^{-/-}$ mice were reduced by 45% and 48%, respectively, as compared to those developed in the liver of *Wt* mice (Figure 4A,B). Additionally, the extracellular matrix of mouse HCCs originating in *hHIF-2α*$^{-/-}$ mice also had a significant lower prevalence of α-SMA positive

myofibroblasts as compared to that of the tumors arising in *Wt* control mice (Figure 5A). This was accompanied by a significant reduction in the mRNA levels of MMP-9 and α-SMA (Figure 5B,C) and by a trend for decreased collagen Sirius Red staining (Figure 5D), despite the differences did not reach statistical significance. Altogether, these data suggested that the hepatocyte-specific deletion of HIF-2α might affect tumor growth and impact on the formation of extracellular matrix within the tumor, making the microenvironment less favorable for tumor progression. On the other hand, parameters related to inflammatory response were found to be significantly decreased in the tumors detected in *hHIF-2α*$^{-/-}$ mice vs those in *Wt* mice, including macrophage infiltration, detected by immunohistochemistry (IHC) (Figure 6A) and transcript levels for F4/80 (Figure 6B), as well as transcript levels for PD-L1 and IRF4 (Figure 6 C,D). These results, once again suggest that in *hHIF-2α*$^{-/-}$ mice the tumor microenvironment might be less favorable for tumor progression.

Hepatocyte-specific HIF-2α deletion affects HCC proliferative capacity

On the basis of the relevant reduction of both the number and the size of tumor masses that developed in *hHIF-2α*$^{-/-}$ mice we next investigated whether this effect might be related to a modulation in the proliferative capacity of cancer cells. Indeed, literature data indicate that in non-liver tumors HIF-2α has a greater oncogenic capacity than HIF-1α, being able to promote tumor proliferation, stemness and radio- and chemo-resistance. [16,19,26-28] The transcriptional analysis of the specimens obtained from tumor and peritumoral tissue of *Wt* mice showed that the transcripts of the cell proliferation markers PCNA (proliferating cell nuclear antigen) and nuclear antigen Ki67 were significantly increased in the tumor masses (Figure 7A,C) and positively correlated with that of HIF-2α (Figure 7B,D). Consistently, the lack of HIF-2α resulted in a decreased PCNA and Ki67 expression in mouse HCCs, without affecting the expression of these markers in peritumoral areas (Figure 7A,C). IHC analysis confirmed a selective reduction in PCNA staining (Figure 8A) as well as a significant decrease in transcript levels for Cyclin E1 (CCNE1) and Cyclin E2 (CCNE2) in the tumors from *hHIF-2α*$^{-/-}$ mice (Figure 8B). At protein level, PCNA reduction was accompanied by a concomitant increase in the cellular content of the cell cycle inhibitors p53 and p21 (Figure 9A-C). Previous studies have evidenced that HIF-2α can positively regulate c-Myc expression which, in turn, directly stimulates PCNA production in HCC cells under hypoxic conditions, thus promoting cancer cell proliferation and HCC resistance to the tyrosine

kinase inhibitor Sorafenib. [29,30] Accordingly, we observed that c-Myc mRNA levels in mouse HCCs from *Wt* mice positively correlated (r=0.72; p= 0.008; 95% CI: 0.25-0.92) with those of HIF-2α (Figure 9D). In line with the reduction in cell proliferation, c-Myc mRNA and protein levels were significantly lowered in the tumors developed in *hHIF-2α*$^{-/-}$ mice (Figure 9E,F). Such an effect was apparently unrelated to the modulation of signal pathways involving ERK1/2, JNK and AKT (Figure 10A-C).

HIF-2α overexpression supports *HepG2* cell growth *in vitro*

To investigate the role of HIF-2α in HCC growth we performed cell culture experiments employing *HepG2* cells stably transfected in order to overexpress HIF-2α (*H/2α* cells) as well as related control cells transfected with the empty pCMV6 vector (*H/V6* cells). Figure 11A shows that in *H/2α* cells HIF-2α protein levels increased in a time-dependent manner along with transcripts of HIF-2α target genes such as the chemokine receptor CXCR4 and EPO (Figure 11B). Furthermore, BrdU incorporation assay, cell count and crystal violet assay indicated that *H/2α* cells had a more proliferative phenotype as compared to *H/V6* cells (Figure 11C-E). This was further confirmed by flow cytometry analysis of cell cycle, which outlined a significant shift towards the S phase in the *H/2α* cells (Figure 11F). These changes were accompanied by increased expression of PCNA and c-Myc oncogene in *H/2α* cells as compared to control *H/V6* cells and by a parallel reduction in the levels of cell cycle inhibitor p53 and p21 (Figure 11A).

HIF-2α over-expression associates to SerpinB3 production in either human or experimental NAFLD-associated HCC

In order to confirm and detail the involvement of HIF2α in NAFLD-associated liver carcinogenesis we next performed IHC analysis on human specimens obtained from a cohort of 27 well characterized NAFLD-derived HCC patients (G2 and G3 grading) (Figure 12A). In these tumors HIF-2α staining was detectable in 67% of the samples (18 out 27) with 11 samples (61%) showing intense positivity and 7 (39%) moderate staining (Figure 12A). Furthermore, 9 out of 11 (82%) HCC samples with intense HIF-2α staining in the cytoplasm were also characterized by HIF-2α nuclear positivity, although the number of positive nuclei varied within patients and in different areas of the same specimens. Weak HIF-2α nuclear positivity was occasionally seen in some samples from

tumors displaying moderate HIF-2α cytoplasm positivity. Conversely, the nuclei of non-parenchymal cells, mainly inflammatory cells or myofibroblast-like cells in fibrotic septa, were negative for HIF-2α (Figure 12A). HIF-2α positivity was prevalent in HCCs developing in cirrhotic livers (14 out of 16; 88%) as compared to HCCs arising in non-cirrhotic livers (3 out of 10; 30%) and HIF-2α nuclear expression was strongly associated (OR=16.33; 95% CI 2.2-121.5; p=0.0085) with the presence of cirrhosis (Figure 12B). HIF-2α expression in HCCs was also associated with a trend for lower survival and an earlier tumor recurrence as compared to patients with undetectable HIF-2α (Figure 12C,D). However, these differences did not reach the statistical significance likely because the limited number of patients recruited.

IHC analysis of NAFLD-related HCCs also showed a strict association between HIF-2α and the expression of SerpinB3 (SB3), a HIF-2α-dependent cysteine-proteases inhibitor that has been involved in stimulating proliferation, epithelial-to-mesenchymal transition (EMT) and invasiveness in liver cancer cells. [31] In fact, 10 out 11 (90%) tumors positive for HIF-2α displayed intense (n=7) or moderate (n=3) cytoplasmic staining for SB3 (Figure 13A), whereas the remaining HIF-2α-negative specimens were largely negative (n= 11) or weakly positive (n=5) for SB3. In the same way, we found a strong linear correlation between HIF-2α and SB3 mRNAs (r=0.61; p=0.03; 95%CI 0.06-0.87) in the individual NAFLD-related HCC induced in *Wt* mice (Figure 13B), while SB3 levels were significantly decreased at both transcript and protein levels in the tumors from *hHIF-2α*$^{-/-}$ mice (Figure 13C,D).

YAP influences c-Myc activity in NAFLD-related HCCs

Growing evidence points out the involvement/activation of Hippo pathway in liver carcinogenesis. [32-37] In particular, the Hippo-dependent transcriptional factor YAP (Yes-associated protein) has been shown to contribute to c-Myc activation in HCCs. [33] According to Turato and co-workers [38] SB3 can modulate c-Myc activity by inhibiting its degradation by calpain as well as by stimulating the Hippo pathway through an enhanced expression of YAP. Since we have observed that SB3 up-upregulation was strictly linked to HIF-2α stimulation in both human and rodent NAFLD-related HCCs, we next investigated whether YAP might account for high expression of c-Myc in WT tumors. We observed that YAP transcripts in individual NAFLD-derived HCC developed in WT mice directly correlated (r=0.666; p=0.013; 95% CI: 0.18-0.89) with HIF-2α expression, whereas a significant lowering of YAP protein levels was evident in tumors from mice lacking HIF-2α (Figure

14A,B) in parallel with SB3 down-modulation. To better investigate the involvement of YAP in supporting HIF-2α-mediated carcinogenesis we went back to *HepG2* cells stably overexpressing HIF-2α (*H/2α* cells). In this setting we observed that YAP was up-regulated in a time dependent manner in *H/2α* cells (Figure 14C) and that the treatment of *H/2α* cells with a specific YAP siRNA was able to reduce the expression of c-Myc at the levels observed in control cells receiving scrambled siRNA (*H/V6 SC*) (Figure 14D), confirming involvement of YAP in c-Myc expression by HIF-2α. From these data we propose that the activation of hepatocyte HIF-2α has a critical role in liver carcinogenesis during NAFLD evolution by promoting c-Myc activation through pathways that involves SB3 and Hyppo signaling.

Discussion

Hypoxia and HIFs, particularly HIF-1α, have been proposed to play an important role in the progression of CLD and in the development of HCC [7-11,14] but the actual contribution of HIF-2α to HCC development is by far less well characterized. In particular, conflicting results have been reported on the impact of HIF-2α on liver carcinogenesis, particularly on cell survival and proliferation. [15-19] Furthermore, although a previous study has proposed HIF-2α involvement in NAFLD-related HCC, [20] no definitive evidence is so far available on the actual contribution of HIF-2α in the processes leading to liver carcinogenesis.

In the present study we took advantage of mice carrying the selective deletion of hepatocyte HIF-2α (h*HIF-2α*$^{-/-}$) to mechanistically investigate the role of HIF-2α in NAFLD-related HCC. The use of these mice has previously allowed the demonstration of the critical contribution of hepatocyte HIF-2α in the evolution of experimental NAFLD by decreasing parenchymal injury, fatty liver, lobular inflammation, and the development of liver fibrosis. [23]

In this work the induction of HCCs in *hHIF-2α*$^{-/-}$ mice by DEN/NAFLD protocol has shown that the lack of parenchymal HIF-2α halves the number and the size of mouse HCCs as compared to *Wt* mice. Such an effect is associated with a parallel lowering in the expression of proliferative markers PCNA and Ki67 along with an induction of p21 and p53 in cancer cells, indicating that hepatocyte HIF-2α can directly promote cancer cell proliferation and survival. These data are supported by *in vitro* experiments revealing that *HepG2* cells stably overexpressing HIF-2α (*H/2α* cells) display a more proliferative phenotype compared to control cells and a significant shift towards the S phase of the cell cycle. These results are in line with literature data linking HIF-2α

with an enhanced tumor aggressiveness through the promotion of cell proliferation, stemness and radio- and chemo-resistance. [27,28,39-41] Nonetheless we cannot exclude that besides the boosting of cell proliferation, additional mechanisms might be involved in the pro-carcinogenic action of HIF-2α, as we have previously observed that hepatocyte HIF-2α suppression ameliorates hepatic inflammation and fibrosis in NASH livers. [23] Indeed, steatohepatitis not only promotes carcinogen-induced HCCs, [42] but also leads to their spontaneous development in mice fed with NASH-inducing choline deficient diet. [43,44] Moreover, the lack of hepatocyte HIF-2α can reduce both the inflammatory response, as confirmed in this study in HCC from h*HIF-2α*$^{-/-}$ mice (see Figure 6A-D), and the recruitment of cancer associated myofibroblasts which contribute to the development of a permissive tumor microenvironment. [45]

So far, the mechanisms by which HIF-2α can support HCC growth have not been fully characterized because of the interplay between HIF-1α and HIF-2α observed in HCC cell lines, [46,47] and the fact that, depending on the cell context, HIF-2α overexpression could have anti-proliferative and pro-apoptotic actions in HCCs. [19] HIF-2α up-regulation has been reported as a common mechanism in the development of HCC resistance to the multi-kinase inhibitor Sorafenib. [48] In these settings, HIF-2α promoted cell survival by stimulating the signaling of TGF-α/ EGFR pathway and by inducing cyclin D1, β-catenin and c-Myc expression. [48] Here we show that, at variance with what observed in HCC spheroids, [46] the up-regulation of HIF-2α in NAFLD-derived HCCs does not affect HIF-1α levels. Moreover, in both *HepG2* cells and mouse HCCs HIF-2α expression associates with a stimulation in c-Myc production. Such an effect does not seem to involve signaling through AKT, ERK1/2, JNK pathways, but appears mediated by YAP signaling. We observed, in fact, that YAP and HIF-2α transcript levels were positively correlated, and that hepatocyte HIF-2α deletion significantly affected both YAP and c-Myc content of murine tumors. Moreover, in tumors from *hHIF-2α*$^{-/-}$ mice, we detected a significant decrease of transcript levels of CCNE1 and CCNE2, two cyclins that have been described to have an important role for HCC progression and to synergistically impair overall survival in HCC patients [49]. In line with these findings, YAP is up-regulated in *H/2α* cells. The capacity of YAP to sustain c-Myc activity in HCCs is consistent with the report by Xiao et al. [33] who observed that c-Myc and YAP proteins are closely correlated in human liver cancers with YAP promoting c-Myc transcriptional output through c-Abl. Furthermore, Ma and coworkers have recently reported that HIF-2α stimulates colon cancer cell growth by up-regulating YAP activity through a mechanism independent from Src, PI3K, ERK1/2, or MAPK pathways. [40] On these bases, we propose that HIF-2α activation can promote HCC growth by

sustaining YAP/c-Myc interaction. Such a hypothesis does not exclude other pro-tumorigenic actions of HIF-2α as, for instance, the stimulation of long non-coding RNA NEAT1 (Nuclear-Enriched Abundant Transcript 1) enzyme, which has recently been implicated in sustaining EMT and migration of HCC cells. [41] Concerning the mechanisms by which HIF-2α can modulate YAP, we have previously shown a role for SB3.[38] Although SB3 is virtually undetectable in normal human livers, its expression is well evident in liver biopsies from patients with CLD and in a fraction of HCCs. [50,51] In HCC cells SB3 is specifically regulated by HIF-2α, [31] while, on its turn, SB3 enhances HIF-2α transcriptional activity by promoting its stabilization through the conjugation with NEDD8 (Neural precursor cell Expressed Developmentally Downregulated-8) induced by NAE1 (NEDD8-E1 activating enzyme). [26]

Data obtained in human NAFLD-related HCC specimens support the observations in experimental models. We have detected HIF-2α over-expression in two third of human HCC developing in NAFLD patients with a strong positive association (OR=16.33) between HIF-2α nuclear localization and HCC development in cirrhotic livers, essentially confirming data from a previous study.[20] Of interest, HIF-2α activation and nuclear staining is appreciable already at the early stage of the disease (F0-F1) in about 70% of the NAFLD patients and a similar prevalence is maintained with disease progression to fibrosis/cirrhosis (F3-F4). [23] Our data also suggest that sustained high HIF-2α expression associates with a trend for shorter survival and earlier tumor recurrence in line with the poor patient outcome observed in others HIF-2α expressing tumors [27,28,39] and in agreement with the decreased survival previously reported in NAFLD-related HCC patients. [20]
Additional data obtained in the cohort of NAFLD-related HCC analyzed in this study indicate that intranuclear HIF-2α associated with an enhanced expression of SB3. Such a prevalence of SB3 positivity in human HCC is higher than that of 22% previously observed in a group of HCCs with other etiologies, mainly viral, [38] indicating that SB3 induction represents a specific response to HIF-2α activation in NAFLD-associated HCCs. Consistently, SB3 is significantly down-regulated in mouse HCCs from *hHIF-2α*$^{-/-}$ mice in parallel with the lowering of both YAP and c-Myc. This suggests that indeed SB3 might be involved in modulating HIF-2α/YAP/c-Myc axis in order to sustain cell growth in NAFLD-associated HCCs. Nonetheless, we cannot exclude alternative mechanisms since, for example, the orphan G protein-coupled receptor GPRC5A has been shown to mediate HIF-2α/YAP interaction in colon cancer cells. [52]

In conclusion, our results indicate that HIF-2α over-expression seems to be a specific feature in NAFLD-related HCCs and might significantly contribute to sustain the tumor development in NAFLD patients. These observations, along with the notions that interference with HIF-2α counteract HCC resistance to Sorafenib [53] and radiation treatment, [54] suggest the possibility of using HIF-2α-blocking drugs as a therapeutic intervention for a tumor that, at present, has few curative options.

Material & Methods

Materials:

Enhanced chemiluminescence (ECL) reagents and nitrocellulose membranes (Hybond-C extra) were from Amersham Pharmacia Biotech Inc. (Piscataway, NJ, USA). The following antibodies were used: anti-HIF-1α (NB100-479) and anti-HIF-2α (NB100-122) from Novus Biologicals (Cambridge, UK); anti CD105 (PA5-12511), anti PCNA (PA5-27214) and anti-SB3 (PA5-30164) from ThermoFisher Scientific (Rockford, IL, USA); anti-α-SMA (M0851) was from DAKO (Agilent, St Clara, CA, USA); anti-SB3 (GTX32866) from GeneTex (Irvine, Ca, USA); anti-F4/80 (14-4801-82) from E-Bioscience (Affymetrix, St Clara, CA, USA); anti-YAP(sc-15407), anti-c-MYC (sc-788), anti-SB3 (sc21767), anti-p53 (sc-6243), anti-p21 (sc-817), anti-ERK (sc-94), anti-JNK (sc-571), anti-vinculin (sc-73614), anti-p-Akt1/2/3 (sc-7985-R), anti-Akt1/2/3 (sc-8312) from Santa Cruz Biotechnology; anti-P-ERK (#4696), anti-P-JNK (#9255) from Cell Signaling Technology; anti-β-actin (A5441) from Sigma Aldrich. HiPerfect Transfection Reagent was from Qiagen, Lipofectamine 2000 (Invitrogen-Life Technologies), Plasmid DNA purification NucleoBond XtraMIDI (Macherey-Nagel, Germany), pCMV6-Entry vectors (Origene, Rockville, MD).

Human Subjects

For this study we analyzed liver specimens from 27 NAFLD patients with HCC (Edmonson-Steiner G2 and G3 grade) referring to the Division of Gastro-Hepatology of the University of Turin. All samples were collected at the time of resection or transplantation. All subjects gave informed consent to the analysis and the study protocol, conformed to the ethical guidelines of the 1975 Declaration of Helsinki, was approved by the ethics' committee of the Azienda Ospedaliera

Universitaria Città della Salute, Torino, Italy. The clinical and biochemical features of the patients are reported in Table 1.

Animal experimentation

Mice carrying a hepatocyte-specific deletion of HIF-2α (*hHIF-2α*$^{-/-}$ mice) were obtained by breeding *HIF-2α*$^{fl/fl}$ *C57BL/6* mice with mice on the same genetic background expressing the Cre-recombinase under the control of the Albumin promoter (*Alb/Cre*$^{+/+}$ *mice*) (Jackson Laboratories, Bar Harbor, Maine, USA). [23] NAFLD-associated liver carcinogenesis was induced, in male *hHIF-2α*$^{-/-}$ mice (n=6) and related control sibling littermates not carrying HIF-2α deletion (*Wt,* n=9), with an established experimental protocol involving a single administration of DEN (diethyl nitrosamine, 25 mg/kg bw, i.p.) at the age of 2 weeks followed by the feeding with a CDAA (choline-deficient L-aminoacid-defined) diet (Laboratorio Dottori Piccioni, Gessate, Italy) for 25 weeks starting from the age of 6 weeks. [24] At the time of the sacrifice the livers of the animals were collected, measured, photographed and the number of visible HCC tumor masses on the surface of the livers were counted and measured with a caliper. For each animal the two biggest tumor masses were isolated and collected for specific analysis. In preliminary experiments eight weeks old male *hHIF-2α*$^{-/-}$ mice (n=8) and related control sibling littermates not carrying HIF-2α deletion (*Wt,* n=8) were fed with the corresponding choline sufficient diet (CSAA) for 12 or 24 weeks. The experiments complied with national ethical guidelines for animal experimentation and the experimental protocols were approved by the Italian Ministry of Health.

Cell lines and culture conditions

HepG2 cells (American Type Culture Collection, USA) were used and maintained in Dulbecco's modified Eagle's medium supplemented with 10% fetal-bovine serum, 100 U/ml penicillin, 100 µg/ml streptomycin and 25 µg/ml amphotericin-B, as previously reported. [31] The pCMV6-based mammalian expression vectors, empty (used as a control) and encoding HIF-2α (OriGene, Rockville, MD), were used in order to generate and select *HepG2* cells stably overexpressing HIF-2α [31]. *HepG2* cells were seeded and then transfected 24 hr later with 10 µg of each vector using Lipofectamine 2000 (Invitrogen, Carlsbad, CA). HIF-2α expression of the generated stable

transfectants was carefully characterized, after which the cell lines carrying the empty vector (*H/V6*) and overexpressing HIF-2α (*H/2α*) were then used for the experiment described.

H/2α and control cells containing the empty pCMV6 vector (*H/V6*) were grown in Dulbecco's modified Eagle's medium under normoxic conditions to obtain the desired sub-confluence level (65-70%).

Western Blot analysis

Total cell/tissue lysates, obtained as previously described [23,26,31], were subjected to sodium dodecyl sulfate-polyacrylamide gel-electrophoresis on 12%, 10% or 7.5% acrylamide gels, incubated with desired primary antibodies, then with peroxidase-conjugated anti-mouse or anti-rabbit immunoglobulins in Tris-buffered saline-Tween containing 2% (w/v) non-fat dry milk and finally developed with the ECL reagents according to manufacturer's instructions. Sample loading was evaluated by reblotting the same membrane with antibodies raised against β-actin or vinculin.

*Quantitative real-time PCR (*Q-PCR*)*

RNA extraction, complementary DNA synthesis, quantitative real-time PCR (Q-PCR) reactions were performed on cells samples, murine liver specimens and on two HCC tumor masses isolated from each murine liver as previously described [23,26]. mRNA levels were measured by Q-PCR, using the SYBR® green method as described. [23] More details and oligonucleotide sequences of primers used for Q-PCR are available in Table 2.

Immunohistochemistry, Sirius Red staining and histo-morphometric analysis

Paraffin-embedded human liver specimens and/or murine liver specimens used in this study were immuno-stained as previously reported. [23,26,31] Briefly, paraffin sections (4 µm thick), mounted on poli-L-lysine coated slides, were incubated with the monoclonal antibody against HIF-1α (dil. 1:100 v/v), HIF-2α (dil. 1:200 v/v), α-SMA (dil. 1:400, v/v), PCNA (dil. 1:400 v/v), F4/80 (dil. 1:500 v/v), SB3 (dil. 1:50 v/v). After blocking endogenous peroxidase activity with 3% hydrogen peroxide and performing microwave antigen retrieval, primary antibodies were labeled by using EnVision, HRP-labeled System (DAKO) and visualized by 3'-diaminobenzidine substrate. Collagen deposition was

evidenced by Picro-Sirius Red staining as previously described [23] and quantification of fibrosis in the murine liver was performed by histo-morphometric analysis using a digital camera and a bright field microscope to collect images that were then analyzed by employing the ImageJ software.

Cell proliferation assays

Proliferation of *H/V6* or *H/2α* cells was evaluated by crystal violet assay by seeding cells in a 96-well plate at a density of 10^4 cells per well up to 72 hrs. At the desired time, the medium was removed, and the cells were washed twice with phosphate-buffered saline, once with distilled water and then stained with 0.5% (w/v) crystal violet solution for 20 min. After washing with water, the crystal violet was solubilized with 50 µl of 10% acetic acid solution, and absorbance was measured at 595–650 nm using a microplate reader (SpectraMAX M3; Molecular Devices, Sunnyvale, CA, USA). The proliferative capacity of *H/V6* or *H/2α* cells was further confirmed by Bromo deoxyuridine (BrdU) incorporation assay using a colorimetric kit supplied by Roche Diagnostic (11647229001).

Cell cycle analysis

Cell cycle analysis was performed essentially as recently reported. [26] Briefly, *H/V6* and *H/2α* cells were seeded in culture plates (10^5 cells per well, 35 mm Ø), up to 72 hrs. At indicated time point cells were trypsinized, centrifuged at 1000 rpm for 10 min and fixed with ethanol (ET-OH 70%), then treated with RNAse for 30 min (final concentration 0.4 mg/ml) and stained with propidium iodide (final concentration 0.184 mg/ml). The cell cycle was analysed by flow cytometry (Accuri C6 flow cytometer, Becton & Dickinson, Milan, Italy) and quantified with FCS Express 4 Flow Research Edition software.

YAP Silencing by Small RNA Interference

RNA interference experiments to knockdown YAP expression in *H/V6* or *H/2α* were performed using siRNA duplex and HiPerfect Transfection reagent (Qiagen Italia, Milano, Italy) according to

manufacturer's instructions up to 72 hrs, as previously described. [34] The following target sequence was used:

YAP: 5'CAGGTGATACTATCAACCAAA 3'

Data analysis and statistical calculations

Statistical analyses were performed by GraphPad Prism 6.01 statistical software (GraphPad Software, San Diego, CA, USA) using one-way ANOVA test with Tukey's correction for multiple comparisons, Student's t test or Mann-Whitney test for non-parametric values. Significance was taken at the 5% level. Normality distribution was assessed by the Kolmogorov-Smirnov algorithm. Associations were estimated using Pearson correlation and Fisher's exact test for the contingency analysis. Kaplan–Meier curves of survival and time to recurrence were estimated using log-rank (Mantel–Cox) test. The data from cell culture experiments represent means ± SEM of at least three independent experiments.

All authors had access to the study data and had reviewed and approved the final manuscript.

REFERENCES

1. Younossi Z, Tacke F, Arrese M, Chander Sharma B, Mostafa I, Bugianesi E, Wong VW-S, Yilmaz Y, George J, Fan J, Vos M. Global Perspectives on Nonalcoholic Fatty Liver Disease and Nonalcoholic Steatohepatitis. Hepatology 2019;69:2672-82.

2. McPherson S, Hardy T, Henderson E, Burt AD, Day CP, Anstee QM. Evidence of NAFLD progression from steatosis to fibrosing-steatohepatitis using paired biopsies: Implications for prognosis and clinical management. J Hepatol 2015;62:1148-55.

3. Younossi ZM, Golabi P, de Avila L, Minhui Paik J, Srishord M, Fukui N, Qiu Y, Burns L, Afendy A, Nader F. The Global Epidemiology of NAFLD and NASH in Patients with type 2 diabetes: A Systematic Review and Meta-analysis. J Hepatol 2019; pii: S0168-8278(19)30393-9.

4. Torres DM, Harrison SA. Nonalcoholic steatohepatitis and noncirrhotic hepatocellular carcinoma: fertile soil. Semin Liver Dis 2012;32:30-8.

5. Younes R, Bugianesi E. Should we undertake surveillance for HCC in patients with NAFLD? J Hepatol 2018;68:326-34.

6. Younossi Z, Stepanova M, Ong JP, Jacobson IM, Bugianesi E, Duseja A, Eguchi Y, Wong VW, Negro F, Yilmaz Y, Romero-Gomez M, George J, Ahmed A, Wong R, Younossi I, Ziayee M, Afendy A. Nonalcoholic Steatohepatitis Is the Fastest Growing Cause of Hepatocellular Carcinoma in Liver Transplant Candidates. Global Nonalcoholic Steatohepatitis Council. Clin Gastroenterol Hepatol 2019;17:748-55.e3.

7. Nath B, Szabo G. Hypoxia and hypoxia inducible factors: diverse roles in liver diseases. Hepatology 2012;55:622-633.

8. Wilson GK, Tennant DA, McKeating JA. Hypoxia inducible factors in liver disease and hepatocellular carcinoma: current understanding and future directions. J Hepatol 2014 ;61:1397-1406.

9. Lefere S, Van Steenkiste C, Verhelst X, Van Vlierberghe H, Devisscher L, Geerts A. Hypoxia - regulated mechanisms in the pathogenesis of obesity and non-alcoholic fatty liver disease. Cell. Mol Life Sci 2016; 73:3419-3431.

10. Chen C, Lou T. Hypoxia inducible factors in hepatocellular carcinoma. Oncotarget 2017;8:46691-703.

11. McKeown SR. Defining normoxia, physoxia and hypoxia in tumours-implications for treatment response. Br J Radiol 2014; 87:20130676.

12. Majmundar AJ, Wong WJ, Simon MC. Hypoxia-inducible factors and the response to hypoxic stress. Mol Cell 2010;40:294-309. doi: 10.1016/j.molcel.2010.09.022.

13. Schito L, Semenza GL. Hypoxia-Inducible Factors: Master Regulators of Cancer Progression. Trends Cancer 2016; 2:758-70.

14. Luo D, Wang Z, Wu J, Jiang C, Wu J. The role of hypoxia inducible factor-1 in hepatocellular carcinoma. Biomed Res Int 2014; 2014:409272.

15. Menrad H, Werno C, Schmid T, Copanaki E, Deller T, Dehne N, Brune B. Roles of hypoxia-inducible factor-1alpha (HIF-1alpha) versus HIF-2alpha in the survival of hepatocellular tumor spheroids. Hepatology 2010; 51:2183–92.

16. He C, Sun XP, Qiao H, Jiang X, Wang D, Jin X, Dong X, Wang J, Jiang H, Sun X. Downregulating hypoxia-inducible factor-2alpha improves the efficacy of doxorubicin in the treatment of hepatocellular carcinoma. Cancer Sci 2012;103:528–34.

17. Sun HX, Xu Y, Yang XR, Wang WM, Bai H, Shi RY, Naya SK, Devbhandari RP, He Y, Zhu Q-F, Sun Y-F, Hu B, Khan M, Anders RA, Fan J. Hypoxia inducible factor 2 alpha inhibits hepatocellular carcinoma growth through the transcription factor dimerization partner 3/ E2F transcription factor 1-dependent apoptotic pathway. Hepatology 2013; 57:1088-97.

18. Zhao D, Zhai B, He C, Tan G, Jiang X, Pan S, Dong X, Wei Z, Ma L, Qiao H, Jiang H, Sun X. Upregulation of HIF-2alpha induced by sorafenib contributes to the resistance by activating the TGF-alpha/EGFR pathway in hepatocellular carcinoma cells. Cell Signal 2014; 26:1030–1039.

19. Yang SL, Liu LP, Niu L, Sun YF, Yang XR, Fan J, Ren J-W, Chen GG, Lai PBS. Downregulation and pro-apoptotic effect of hypoxia-inducible factor 2 alpha in hepatocellular carcinoma. Oncotarget 2016;7:34571-81.

20. Chen J, Huang J, Li Z, Gong Y, Zou B, Liu X, Ding L, Li P, Zhu Z, Zhang B, Guo H, Cai C, Li J. HIF-2α upregulation mediated by hypoxia promotes NAFLD-HCC progression by activating lipid synthesis via the PI3K-AKT-mTOR pathway. Aging 2019;11:10839-60.

21. Rankin EB, Rha J, Selak MA, Unger TL, Keith B, Liu Q, Haase VH. Hypoxia-inducible factor 2 regulates hepatic lipid metabolism. Mol Cell Biol 2009;29:4527-38.

22. Qu A, Taylor M, Xue X, Matsubara T, Metzger D, Chambon P, Gonzalez FJ, Shah YM. Hypoxia-inducible transcription factor 2α promotes steatohepatitis through augmenting lipid accumulation, inflammation, and fibrosis. Hepatology 2011;54:472-83.

23. Morello E, Sutti S, Foglia B, Novo E, Cannito S, Bocca C, Rajsky M, Bruzzì S, Abate ML, Rosso C, Bozzola C, David E, Bugianesi E, Albano E, Parola M. Hypoxia-inducible factor 2α drives nonalcoholic fatty liver progression by triggering hepatocyte release of histidine-rich glycoprotein. Hepatology 2018 Jun;67(6):2196-2214.

24. Ma C, Kesarwala AH, Eggert T, Medina-Echeverz J, Kleiner DE, Jin P, Stroncek DF, Terabe M, Kapoor V, ElGindi M, Han M, Thornton AM, Zhang H, Egger M, Luo J, Felsher DW, McVicar DW, Weber A, Heikenwalder M, Greten TF. NAFLD causes selective CD4(+) T lymphocyte loss and promotes hepatocarcinogenesis. Nature 2016;531:253-57.

25. Salomao M, Remotti H, Vaughan R, Siegel AB, Lefkowitch JH, Moreira RK. The steatohepatitic variant of hepatocellular carcinoma and its association with underlying steatohepatitis. Hum Pathol 2012; 43:737-746.

26. Cannito S, Foglia B, Villano G, Turato C, Delgado TC, Morello E, Pin F, Novo E, Napione L, Quarta S, Ruvoletto M, Fasolato S, Zanus G, Colombatto S, Lopitz-Otsoa F, Fernández-Ramos D, Bussolino F, Sutti S, Albano E, Martínez-Chantar ML, Pontisso P, Parola M. SerpinB3 differently up-regulates hypoxia inducible factors -1α and -2α in hepatocellular carcinoma: mechanisms revealing novel potential therapeutic targets. Cancers 2019; 11:E1933.

27. Koh MY, Lemos R Jr, Liu X, Powis G. The hypoxia-associated factor switches cells from HIF-1α- to HIF-2α-dependent signaling promoting stem cell characteristics, aggressive tumor growth and invasion. Cancer Res 2011;71:4015-27.

28. Keith B, Johnson RS, Simon MC. HIF-1α and HIF-2α: sibling rivalry in hypoxic tumour growth and progression. Nat Rev Cancer 2011;12:9-22.

29. Liu F, Dong X, Lv H, Xiu P, Li T, Wang F, Xu Z, Li J. Targeting hypoxia-inducible factor-2α enhances sorafenib antitumor activity via β-catenin/C-Myc-dependent pathways in hepatocellular carcinoma. Oncol Lett 2015;10:778-84.

30. Méndez-Blanco C, Fondevila F, García-Palomo A, González-Gallego J, Mauriz JL. Sorafenib resistance in hepatocarcinoma: role of hypoxia-inducible factors. Exp Mol Med 2018;50:134.

31. Cannito S, Turato C, Paternostro C, Biasiolo A, Colombatto S, Cambieri I, Quarta S, Novo E, Morello E, Villano G, Fasolato S, Musso T, David E, Tusa I, Rovida E, Autelli R, Smedile A, Cillo U, Pontisso P, Parola M. Hypoxia up-regulates SERPINB3 through HIF-2α in human liver cancer cells. Oncotarget 2015; 6:2206-21.

32. Zhang S, Zhou D. Role of the transcriptional coactivators YAP/TAZ in liver cancer. Curr Opin Cell Biol 2019;61:64-71.

33. Xiao W, Wang J, Ou C, Zhang Y, Ma L, Weng W, Pan Q, Sun F. Mutual interaction between YAP and c-Myc is critical for carcinogenesis in liver cancer. Biochem Biophys Res Commun 2013;439:167-72.

34. Tao J, Calvisi DF, Ranganathan S, Cigliano A, Zhou L, Singh S, Jiang L, Fan B, Terracciano L, Armeanu-Ebinger S, Ribback S, Dombrowski F, Evert M, Chen X, Monga SPS. Activation of β-catenin and Yap1 in human hepatoblastoma and induction of hepatocarcinogenesis in mice. Gastroenterology. 2014;147(3):690-701.

35. Perra A, Kowalik MA, Ghiso E, Ledda-Columbano GM, Di Tommaso L, Angioni MM, Raschioni C, Testore E, Roncalli M, Giordano S, Columbano A. YAP activation is an early event and a potential therapeutic target in liver cancer development. J Hepatol. 2014;61(5):1088-96.

36. Moon H, Cho K, Shin S, Kim DY, Han KH, Ro SW. High Risk of Hepatocellular Carcinoma Development in Fibrotic Liver: Role of the Hippo-YAP/TAZ Signaling Pathway. Int J Mol Sci. 2019;20(3):581.

37. Zhu C, Tabas I, Schwabe RF, Pajvani UB. Maladaptive regeneration - the reawakening of developmental pathways in NASH and fibrosis. Nat Rev Gastroenterol Hepatol. 2021;18(2):131-142.

38. Turato C, Cannito S, Simonato D, Villano G, Morello E, Terrin L, Quarta S, Biasiolo A, Ruvoletto M, Martini A, Fasolato S, Zanus G, Cillo U, Gatta A, Parola M, Pontisso P. SerpinB3 and Yap Interplay Increases Myc Oncogenic Activity. Scientific Rep 2015;5:17701.

39. Borovski T, De Sousa E, Melo F, Vermeulen L, Medema JP. Cancer stem cell niche: the place to be. Cancer Res 2011;71:634-39.

40. Ma X, Zhang H, Xue X, Shah YM. Hypoxia-inducible factor 2α (HIF-2α) promotes colon cancer growth by potentiating Yes-associated protein 1 (YAP1) activity. J Biol Chem. 2017;292:17046-17056.

41. Zheng X, Zhang Y, Liu Y, Fang L, Li L, Sun J, Pan Z, Xin W, Huang P. HIF-2α activated lncRNA NEAT1 promotes hepatocellular carcinoma cell invasion and metastasis by affecting the epithelial-mesenchymal transition. J. Cell. Biochem. 2018;119:3247-3256. doi: 10.1002/jcb.26481.

42. Park EJ, Lee JH, Yu GY, He G, Ali SR, Holzer RG, Osterreicher CH, Takahashi H, Karin M. Dietary and genetic obesity promote liver inflammation and tumorigenesis by enhancing IL-6 and TNF expression. Cell 2010;140:197-208.

43. De Minicis S, Agostinelli L, Rychlicki C, Sorice GP, Saccomanno S, Candelaresi C, Giaccari A, Trozzi L, Pierantonelli I, Mingarelli E, Marzioni M, Muscogiuri G, Gaggini M, Benedetti A, Gastaldelli A, Guido M, Svegliati-Baroni G. HCC development is associated to peripheral insulin resistance in a mouse model of NASH. PLoS One 2014;9:e97136.

44. Wolf MJ, Adili A, Piotrowitz K, Abdullah Z, Boege Y, Stemmer K, Ringelhan M, Simonavicius N, Egger M, Wohlleber D, Lorentzen A, Einer C, Schulz S, Clavel T, Protzer U, Thiele C, Zischka H, Moch H, Tschöp M, Tumanov AV, Haller D, Unger K, Karin M, Kopf M, Knolle P, Weber A, Heikenwalder M. Metabolic activation of intrahepatic CD8+ T cells and NKT cells causes nonalcoholic steatohepatitis and liver cancer via cross-talk with hepatocytes. Cancer Cell 2014;26:549-564.

45. Baglieri J, Brenner DA, Kisseleva T. The Role of Fibrosis and Liver-Associated Fibroblasts in the Pathogenesis of Hepatocellular Carcinoma. Int. J. Mol. Sci. 2019;20. pii: E1723.

46. Menrad H, Werno C, Schmid T, Copanaki E, Deller T, Dehne N, Brüne B. Roles of hypoxia-inducible factor-1alpha (HIF-1alpha) versus HIF-2alpha in the survival of hepatocellular tumor spheroids. Hepatology. 2010;51:2183-2192.

47. Xiong XX, Qiu XY, Hu DX, Chen XQ. Advances in Hypoxia-Mediated Mechanisms in Hepatocellular Carcinoma. Mol. Pharmacol. 2017;92:246-255.

48. Zhao D, Zhai B, He C, Tan G, Jiang X, Pan S, Dong X, Wei Z, Ma L, Qiao H, Jiang H, Sun X. Upregulation of HIF-2alpha induced by sorafenib contributes to the resistance by activating the TGF-alpha/EGFR pathway in hepatocellular carcinoma cells. Cell Signal 2014;26:1030–1039.

49. Sonntag R, Giebeler N, Nevzorova YA, Bangen JM, Fahrenkamp D, Lambertz D, Haas U, Hu W, Gassler N, Cubero FJ, Müller-Newen G, Abdallah AT, Weiskirchen R, Ticconi F, Costa IG, Barbacid M, Trautwein C, Liedtke C. Cyclin E1 and cyclin-dependent kinase 2 are critical for initiation, but not for progression of hepatocellular carcinoma. Proc Natl Acad Sci U S A. 2018 Sep 11;115(37):9282-9287.

50. Guido M, Roskams T, Pontisso P, Fassan M, Thung SN, Giacomelli L, Sergio A, Farinati F, Cillo U, Rugge M. Squamous cell carcinoma antigen in human liver carcinogenesis. J. Clin. Pathol. 2008; 61:445–447.

51. Turato C, Vitale A, Fasolato S, Ruvoletto M, Terrin L, Quarta S, Ramirez Morales R, Biasiolo A, Zanus G, Zali N, Tan PS, Hoshida Y, Gatta A, Cillo U, Pontisso P. SERPINB3 is associated with TGF-β1 and cytoplasmic β-catenin expression in hepatocellular carcinomas with poor prognosis. Br. J. Cancer 2014;110: 2708–2715.

52. Greenhough A, Bagley C, Heesom KJ, Gurevich DB, Gay D, Bond M, Collard TJ, Paraskeva C, Martin P, Sansom OJ, Malik K, Williams AC. Cancer cell adaptation to hypoxia involves a HIF-GPRC5A-YAP axis. EMBO Mol Med. 2018;10. pii: e8699.

53. Liu F, Dong X, Lv H, Xiu P, Li T, Wang F, Xu Z, Li J. Targeting hypoxia-inducible factor-2α enhances sorafenib antitumor activity via β-catenin/C-Myc-dependent pathways in hepatocellular carcinoma. Oncol. Lett. 2015;10:778-784.

54. Bertout JA, Majmundar AJ, Gordan JD, Lam JC, Ditsworth D, Keith B, Brown EJ, Nathanson KL, Simon MC. HIF-2alpha inhibition promotes p53 pathway activity, tumor cell death, and radiation responses. Proc. Natl. Acad. Sci. U S A. 2009;106:14391-14396.

Author names in bold designate shared co-first authorship.

Figure Legends

Figure 1. **Experimental NAFLD/NASH-related HCC: the DEN-CDAA murine model.** Graphic representation of the rodent model of NAFLD-associated hepatocarcinogenesis based on a single injection of diethyl-nitrosamine (DEN) at 2 weeks of age and the subsequent induction of steatohepatitis by the administration of a CDAA diet for 25 weeks (**A**). Hematoxylin Eosin staining performed on paraffin-embedded HCC tumor masses from *wild type* mice (Wt) (n = 9) or from

hepatocyte specific HIF-2α *knock-out* mice (hHIF-2α$^{-/-}$) (n = 6). Original magnification as indicated. (**B,C**)

Figure 2. Validation of the DEN-CDAA hepatocyte-specific deletion of HIF-2α murine model. WB analysis of HIF-2α performed in healthy liver of 8 *wild type* mice fed with control diet (Wt CSAA) or in HCC tumor masses from 5 *wild type* mice treated with the DEN-CDAA protocol (Wt DEN-CDAA) (**A**). HIF-2α expression analyzed by Q-PCR (**B**) or WB analysis (**C**) in HCC tumor masses from 9 *wild type* mice (Wt) or from 6 HIF-2α *knock-out* mice (hHIF-2α$^{-/-}$). qPCR analysis of CXCR4 (**D**) and EPO (**E**) transcripts performed in Wt or in hHIF-2α$^{-/-}$. The mRNA values are expressed as fold increase over control values after normalization to the TBP gene expression. Results are expressed as means ± SD. Boxes include the values within 25th and 75th percentile, whereas horizontal bars represent the medians. The extremities of the vertical bars (10th-90th percentile) comprise 80% of the values. Statistical differences were assessed by Student's t test or Mann-Whitney test for non-parametric values (**B,D,E**). For the WB analysis, BIORAD Quantity One software was use to perform the densitometric analysis. Equal loading was evaluated by re-probing membranes for Vinculin or β-actin. Statistical differences were assessed by Student's t test or Mann-Whitney test for non-parametric values (**A**, **C**).

Figure 3. **Hepatocyte-specific deletion of HIF-2α does not affects HIF-1α expression.** Liver expression of HIF-1α evaluated by quantitative real-time PCR (Q-PCR) (**A**) and immunohistochemical analysis (**B**) in HCCs from 9 wild type mice (Wt) or from 6 HIF-2α knock-out mice (hHIF-2α$^{-/-}$). Original magnification as indicated. Gene expression of VEGF, FLK1 and ve-cadherin evaluated by quantitative real-time PCR (q-PCR) in HCC tumor masses from 9 Wt mice or from 6 hHIF-2α$^{-/-}$ mice (**C**). The mRNA values are expressed as fold increase over control values after normalization to the TBP gene expression. Results are expressed as means ± SD. Boxes include the values within 25th and 75th percentile, whereas horizontal bars represent the medians. The extremities of the vertical bars (10th-90th percentile) comprise 80% of the values. Statistical differences were assessed by Student's t test or Mann-Whitney test for non-parametric values. ns: not significant (**C**). WB analysis of cd105 protein levels in HCCs from 7 Wt mice or from 5 hHIF-2α$^{-/-}$ mice (**D**). For the WB analysis, BIORAD Quantity One software was use to perform the densitometric analysis. Equal loading was evaluated by re-probing membranes for β-actin.

Statistical differences were assessed by Student's t test or Mann-Whitney test for non-parametric values. ns: not significant.

Figure 4. Hepatocyte-specific deletion of HIF-2α significantly affects development of experimental liver tumors. Reduction of number and of neoplastic mass measured in HCC tumors (indicated by arrows) from 9 *wild type* mice (Wt) or 6 from HIF-2α *knock-out* mice (hHIF-2α$^{-/-}$) (**A, B**). Results are expressed as means ± SD. Boxes include the values within 25th and 75th percentile, whereas horizontal bars represent the medians. The extremities of the vertical bars (10th-90th percentile) comprise 80% of the values. Statistical differences were assessed by Student's t test (**B**).

Figure 5. **Hepatocyte-specific deletion of HIF-2α significantly affects liver fibrosis.** Liver fibrosis was evaluated morphologically in HCC tumor masses from 9 Wt mice or from 6 hHIF-2α$^{-/-}$ mice, by IHC analysis of α-SMA (**A**) and by Sirius Red Staining (**D**). ImageJ software analysis was performed to evaluate the amount of fibrosis. Data in graphs are expressed as means ± SEM. Statistical differences were assessed by Student's t test or Mann-Whitney test for non-parametric values. ns: not significant. Original magnification as indicated (**A**,**D**). qPCR analysis of α-SMA (**B**) and MMP9 (**C**) transcripts performed in in HCC tumor masses from 9 Wt mice or from 6 hHIF-2α$^{-/-}$ mice. The mRNA values are expressed as fold increase over control values after normalization to the TBP gene expression. Results are expressed as means ± SD. Boxes include the values within 25th and 75th percentile, whereas horizontal bars represent the medians. The extremities of the vertical bars (10th-90th percentile) comprise 80% of the values. Statistical differences were assessed by Student's t test or Mann-Whitney test for non-parametric values. ns: not significant (**B**,**C**).

Figure 6. Hepatocyte-specific deletion of HIF-2α significantly affects the inflammatory response. IHC analysis of F4/80 performed on paraffin-embedded HCC tumor masses from 9 Wt mice or from 6 hHIF-2α$^{-/-}$ mice (**A**). ImageJ software analysis was performed to evaluate the amount of F4/80 positive areas. Data in graphs are expressed as means ± SEM. Statistical differences were assessed by Student's t test or Mann-Whitney test for non-parametric values. Original magnification as indicated (**A**). qPCR analysis of F4/80 (**B**), PD-L1 (**C**), IRF-4 (**D**) transcripts

performed in in HCCs from 9 Wt mice or from 6 hHIF-2α$^{-/-}$ mice. The mRNA values are expressed as fold increase over control values after normalization to the TBP gene expression. Results are expressed as means ± SD. Boxes include the values within 25th and 75th percentile, whereas horizontal bars represent the medians. The extremities of the vertical bars (10th-90th percentile) comprise 80% of the values. Statistical differences were assessed by Student's t test or Mann-Whitney test for non-parametric values (**B**,**C,D**).

Figure 7. HIF-2α expression positively correlates with markers of HCC proliferative capacity. qPCR analysis of PCNA (**A**) and Ki67 (**C**) transcripts performed in peritumoural tissue or HCC tumor masses from 9 *wild type* mice (Wt) or from 6 HIF-2α *knock-out* mice (hHIF-2α$^{-/-}$). The mRNA values are expressed as fold increase over control values after normalization to the TBP gene expression. Results are expressed as means ± SD. Boxes include the values within 25th and 75th percentile, whereas horizontal bars represent the medians. The extremities of the vertical bars (10th-90th percentile) comprise 80% of the values. Statistical differences were assessed by one-way ANOVA test with Tukey's correction for multiple comparisons or Student's t test (**A,C**). Relationship between HIF-2α and PCNA (**B**) or Ki67 (**D**) mRNA in HCCs from 9 *wild type* mice. The values represent the relative mRNA content. The correlation analysis was performed with Pearson r test.

Figure 8. Hepatocyte-specific HIF-2α deletion impact on HCC proliferative capacity. IHC analysis of PCNA performed on paraffin-embedded HCC tumor masses from 9 Wt mice or from 6 hHIF-2α$^{-/-}$ mice (**A**). ImageJ software analysis was performed to evaluate the number of PCNA-positive nuclei per microscopic field. Data in graphs are expressed as means ± SEM. Statistical differences were assessed by Student's t test. Original magnification as indicated (**A**). qPCR analysis of CCNE1 and CCNE2 (**B**) transcripts performed in in HCCs from 9 Wt mice or from 6 hHIF-2α$^{-/-}$ mice. The mRNA values are expressed as fold increase over control values after normalization to the TBP gene expression. Results are expressed as means ± SD. Boxes include the values within 25th and 75th percentile, whereas horizontal bars represent the medians. The extremities of the vertical bars (10th-90th percentile) comprise 80% of the values. Statistical differences were assessed by Student's t test or Mann-Whitney test for non-parametric values (**B**).

Figure 9. Hepatocyte-specific HIF-2α deletion impact on HCC proliferative capacity. WB analysis for PCNA (**A**), p21 (**B**), p53 (**C**) and c-Myc (**F)** performed in HCCs from 6 *wild type* mice (Wt) or from 5 HIF-2α *knock-out* mice (hHIF-2$\alpha^{-/-}$). BIORAD Quantity One software was use to perform the densitometric analysis (data are expressed as Fold Change relative to the normalized Wt expression). Equal loading was evaluated by re-probing membranes for β-actin. Statistical differences were assessed by Student's t test or Mann-Whitney test for non-parametric values (**A,B,C,F**). Relationship between HIF-2α and c-Myc (**D**) mRNA in HCCs from 9 *wild type* mice. The values represent the relative mRNA content. The correlation analysis was performed with Pearson r test. qPCR analysis of c-MYC (**E**) transcript performed in HCCs from 9 Wt mice or from 6 hHIF-2$\alpha^{-/-}$ mice. The mRNA values are expressed as fold increase over control values after normalization to the TBP gene expression. Results are expressed as means ± SD. Boxes include the values within 25th and 75th percentile, whereas horizontal bars represent the medians. The extremities of the vertical bars (10th-90th percentile) comprise 80% of the values. Statistical differences were assessed by Student's t test or Mann-Whitney test for non-parametric values (**E**).

Figure 10. Hepatocyte-specific HIF-2α deletion affects HCC proliferative capacity without the involvement of ERK, JNK, AKT signal pathways. Western blotting analysis of P-AKT (**A**), P-ERK (**B**), P-JNK (**C**) in HCC tumor masses from 9 *wild type* mice (Wt) or from 6 HIF-2α *knock-out* mice (hHIF-2$\alpha^{-/-}$). BIORAD Quantity One software was use to perform the densitometric analysis. Equal loading was evaluated by re-probing membranes for the relative non-phosphorylated protein AKT, ERK, JNK and βActin or vinculin. Results are expressed as means ± SD. Boxes include the values within 25th and 75th percentile, whereas horizontal bars represent the medians. The extremities of the vertical bars (10th-90th percentile) comprise 80% of the values. Statistical differences were assessed by Student's t test or Mann-Whitney test for non-parametric values. ns: not significant.

Figure 11. HIF-2α overexpression support *HepG2* cell growth *in vitro*. WB (Western Blotting) analysis of HIF-2α, c-Myc, PCNA, p53, p21 levels performed on *HepG2* stably transfected in order to overexpress HIF-2α (*H/2α*) or in control *HepG2* cells transfected with empty vector (*H/V6*) at different time point. Equal loading was evaluated by re-probing membranes for β-actin. BIORAD Quantity One software was use to perform the densitometric analysis (data are expressed as Fold Change relative to the normalized *H/V6* expression (**A**). Q-PCR (Quantitative real-time PCR) analysis of CXCR4 and EPO transcripts in *H/2α* or in *H/V6* cells at different time point. Data in

graphs are expressed as means ± SEM. Statistical differences were assessed by one-way ANOVA test with Tukey's correction for multiple comparisons or Kruskal-Wallis test for non-parametric values (**B**). Cell count performed with BrDU Incorporation assay (**C**), Burker chamber (**D**) and Crystal Violet (**E**) techniques performed on *H/2α* or *H/V6* at different time point. Bar graph chart showed the relative quantity of G1, G2 and S ratio in *H/2α* cells compared to the *H/V6* control cells as mean ± SD, resulted from cell cycle analysis by flow cytometry with FCS Express 4 Flow Research Edition software (**F**). These experiments were repeated three separate times, and similar results were obtained.

Figure 12. **Expression of HIF-2α in human NAFLD/NASH-related HCC patients.** IHC analysis of HIF-2α performed on paraffin-embedded human liver specimens from NAFLD/NASH-related HCC patients (n = 27, grade G2-G3). Original magnification as indicated. HIF-2α expression was semi-quantitatively scored blinded, by a pathologist (**A**). Odds ratio meta-analysis is calculated by Fisher's exact test to evaluate the strength of the association between HIF-2α expression and HCC cirrhotic setting (**B**). Kaplan–Meier curves of survival (**C**) and time to recurrence (**D**) according to HIF-2α expression. Statistical analysis was performed using log-rank (Mantel–Cox) test.

Figure 13. SB3 expression correlates with HIF-2α expression in NAFLD/NASH-related HCC patients. IHC analysis of HIF-2α (left panel) or SB3 (right panel) performed on paraffin-embedded human liver specimens from NAFLD/NASH-related HCC patients (n = 27, grade G2-G3). Original magnification as indicated. SB3 expression was semi-quantitatively scored blinded, by a pathologist (Mann-Whitney's U test) (**A**). Relationship between HIF-2α and SB3 mRNA in HCC tumor masses from 9 *wild type* mice. The values represent the relative mRNA content. The correlation analysis was performed with Pearson r test (**B**). qPCR (**C**) and WB (**D**) analysis for SB3 performed in HCC tumor masses from 9 *wild type* mice (Wt) or from 6 HIF-2α *knock-out* mice (hHIF-2$\alpha^{-/-}$) (**C,D**). For the WB analysis, BIORAD Quantity One software was use to perform the densitometric analysis. Equal loading was evaluated by re-probing membranes for β-actin. Statistical differences were assessed by Student's t test or Mann-Whitney test for non-parametric values (**D**). The mRNA values are expressed as fold increase over control values after normalization to the TBP gene expression. Results are expressed as means ± SD. Boxes include the values within 25th and 75th percentile, whereas horizontal bars represent the medians. The extremities of the

vertical bars (10th-90th percentile) comprise 80% of the values. Statistical differences were assessed by Student's t test or Mann-Whitney test for non-parametric values (**C**).

Figure 14. HIF-2α expression directly correlates with YAP. Relationship between HIF-2α and YAP mRNA in HCCs from 9 *wild type* mice. The values represent the relative mRNA content. The correlation analysis was performed with Pearson r test (**A**). WB analysis for YAP performed in HCCs from 9 *wild type* mice (Wt) or from 6 HIF-2α *knock-out* mice (hHIF-2α$^{-/-}$). For the WB analysis, BIORAD Quantity One software was use to perform the densitometric analysis. Equal loading was evaluated by re-probing membranes for β-actin. Statistical differences were assessed by Student's t test or Mann-Whitney test for non-parametric values (**B**). WB analysis of YAP protein levels performed on *HepG2* stably transfected in order to overexpress HIF-2α (*H/2α*) or in control *HepG2* cells transfected with empty vector (*H/V6*) at different time point. Equal loading was evaluated by re-probing membranes for Vinculin (**C**). WB analysis of YAP and c-Myc protein levels performed on *H/2α* or in control *H/V6*, treated or not (SC) with a specific YAP siRNA (siYAP). Equal loading was evaluated by re-probing membranes for β-actin. BIORAD Quantity One software was use to perform the densitometric analysis (data are expressed as Fold Change relative to the normalized *H/V6* expression) (**C,D**).

Table 1

Clinical and biochemical characterization of NAFLD carrying HCC patients investigated**.**

Demographic Data	
Patients Number (Male/Female)	27 (25/2)
Age (Years)	71 (49-86)
BMI	28.2 (22.3-34.6)
Clinical Data	
Hypertension	88.9%

Dyslipidemia (TG>150/HDL<40M / <50 F)	70.4%
Diabetes mellitus	85.2%
CHILD	A (59.3%)
Resection	9/14 (64.3%)
OLT	6 (22.2%)
MELD	9 (6-14)
Biochemical Data	
Triglycerides (mg/dL n.v. 50-150)	111 (77-155)
AST (U/L– n.v. 5–40)	37 (17-83)
ALT (U/L n.v. 5–40)	37 (13-86)
γ-GT (U/L n.v. 5–45)	111 (14-307)
Bilirubin (U/L)	0.9 (0.3-2.5)
AFP (ng/mL n.v. <10)	131.6 (1-2919)
Albumin (g/L)	4.1 (3.3-4.8)
Histological Data	
Steatosis score	0 (18.5%)
	1 (70.4%)
	2 (11.1%)
	3 (3.7%)
Ballooning score	1 (45.5%)
Fibrosis score	1 (40.9%)
Cirrosis	59.3%
NAS score	1-3 (27.3%)
Oncological Data	
N° of Nodules	1 (1-3)

Dimension (mm)	73 (7-180)
Edmondson-Steiner Grading (1-4)	9 (6-14)

The values are expressed as median and inter-quartile range (IQR). For histological scores the range of variability is included.

BMI, body mass index; AST, alanine aminotransferase; ALT, aspartate aminotransferase; γ-GT, gamma-glutamyl transpeptidase; n.v., normal value

Table 2

Oligonucleotide sequences of primers used for Q-PCR**.**

Primer	**Sense**	**Reverse**
murine **CNNE1**	5’ CCCTGGGATGATAATTCAGC 3’	5’ TCTGGGTGGTCTGATTTTCC 3’
murine **CNNE2**	5’ TCTGTGCATTCTAGCCATCG 3’	5’ GTCATCCCATTCCAAACCTG 3’
murine **C-MYC**	5’ CTGTGGAGAAGAGGCAAACC 3’	5’ TTGTGCTGGTGAGTGGAGAC 3’
human **CXCR4**	5’ TCCATTCCTTTGCCTCTTTTGC 3’	5’ ACGGAAACAGGGTTCCTTCAT 3’
murine **CXCR4**	5’ TGGAACCGATCAGTGTGAGT 3’	5’ TTGCCGACTATGCCAGTCAA 3’
murine **Cyp2e1**	5’ TGGGGAAACAGGGTAATGAG 3’	5’ GTGCACAGCCAATCAGAAAG 3’
human **EPO**	5’ GAGCCCAGAAGGAAGCCATC 3’	5’ GCGGAAAGTGTCAGCAGTGA 3’
murine **EPO**	5’ CAGCCACCAGAGACCCTTC 3’	5’ ACATCAATTCCTTCTGAGCTCCC 3’
murine **FLK1**	5’ GGCGGTGGTGACAGTATCTT 3’	5’ GTCACTGACAGAGGCGATGA 3’
murine **F4/80**	5’ GTACAGATGGGGGATGACCAC 3’	5’ GACTGAGTTAGGACCACAAGGTGAG 3’
human **GAPDH**	5’ TGGTATCGTGGAAGGACTCATGAC 3’	5’ ATGCCAGTGAGCTTCCCGTTCAGC 3’
murine **HIF1-α**	5’ TCAAGTTCAGCAACGTGGAAG 3’	5’ TATCGAGGCTGTGTCGACTG 3’
murine **HIF2-α**	5’ AGAGCTGAGGAAGGAGAAATC 3’	5’ ATGTGTCCGAAGGAAGCTG 3’
murine **IRF-4**	5’ GCAGCTCACTTTGGATGACA 3’	5’ CCAAACGTCACAGGACATTG 3’
murine **Ki67**	5’ CATGCAAACCCTCACACTTG 3’	5’ GCTGGTTCCAATTTCTGAGC 3’

murine **MMP9**	5’ CGTCGTGATCCCCACTTACT 3’	5’ AACACACAGGGTTTGCCTTC 3’
murine **PCNA**	5’ CTGTGCAAAGAATGGGGTGAA 3’	5’ AGCAAACGTTAGGTGAACAGG 3’
murine **PD-L1**	5’ AATGCTGCCCTTCAGATCAC 3’	5’ TCAGCGTGATTCGCTTGTAG 3’
murine **SB3**	5’ TTTTACACAAGTCCTTTGTGGAGG 3’	5’ CTGGACACATGGAAGAGACACCAC 3’
murine **TBP**	5’CACATCACAGCTCCCCACCA 3’	5’AGCGGAGAAGATGCTGGAAAC 3’
murine **VE-cadherine**	5’ ATTGAGACAGACCCCAAACG 3’	5’ TTCTGGTTTTCTGGCAGCTT 3’
murine **VEGF-A**	5’ CAGGCTGCTGTAACGATGAA 3’	5’ TTTCTTGCGCTTTCGTTTTT 3’
murine **YAP**	5’ TCAGACAACAACATGGCAGGA 3’	5’ TTCATGGCTGAAGCCGAGTT 3’
murine **αSMA**	5’ CTGACAGAGGCACCACTGAA 3’	5’ CATCTCCAGAGTCCAGCACA 3’

Figure 1

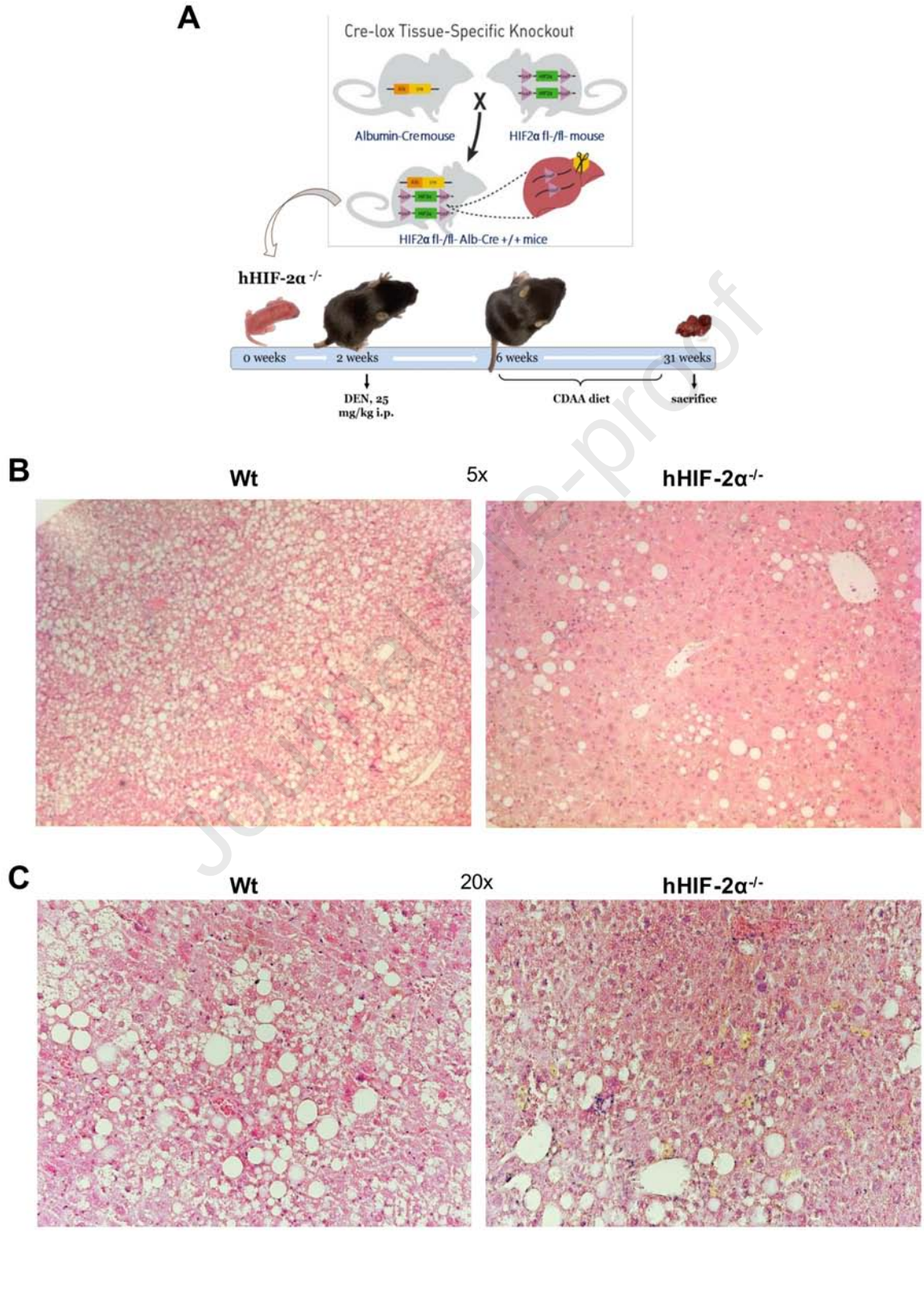

Figure 2

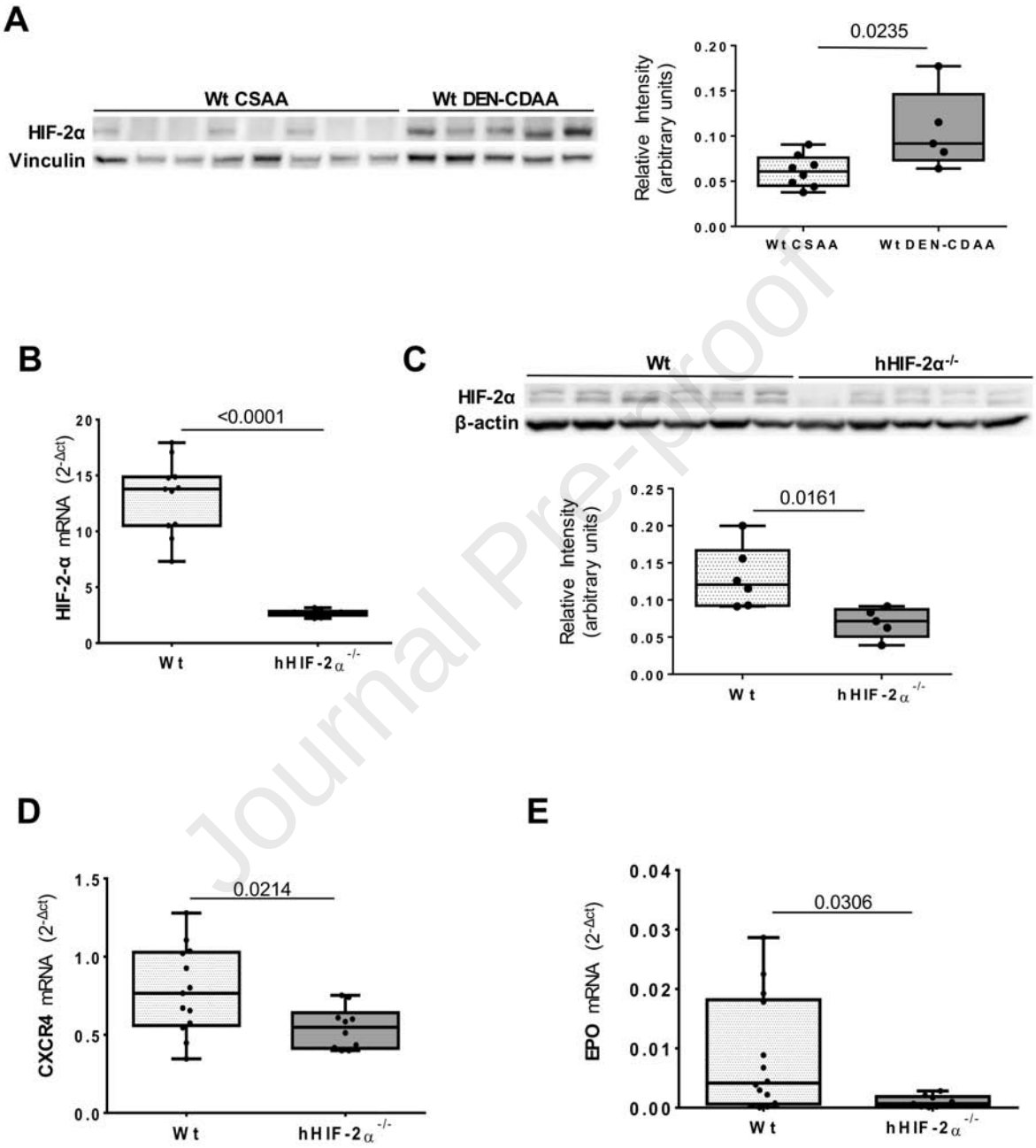

Figure 3

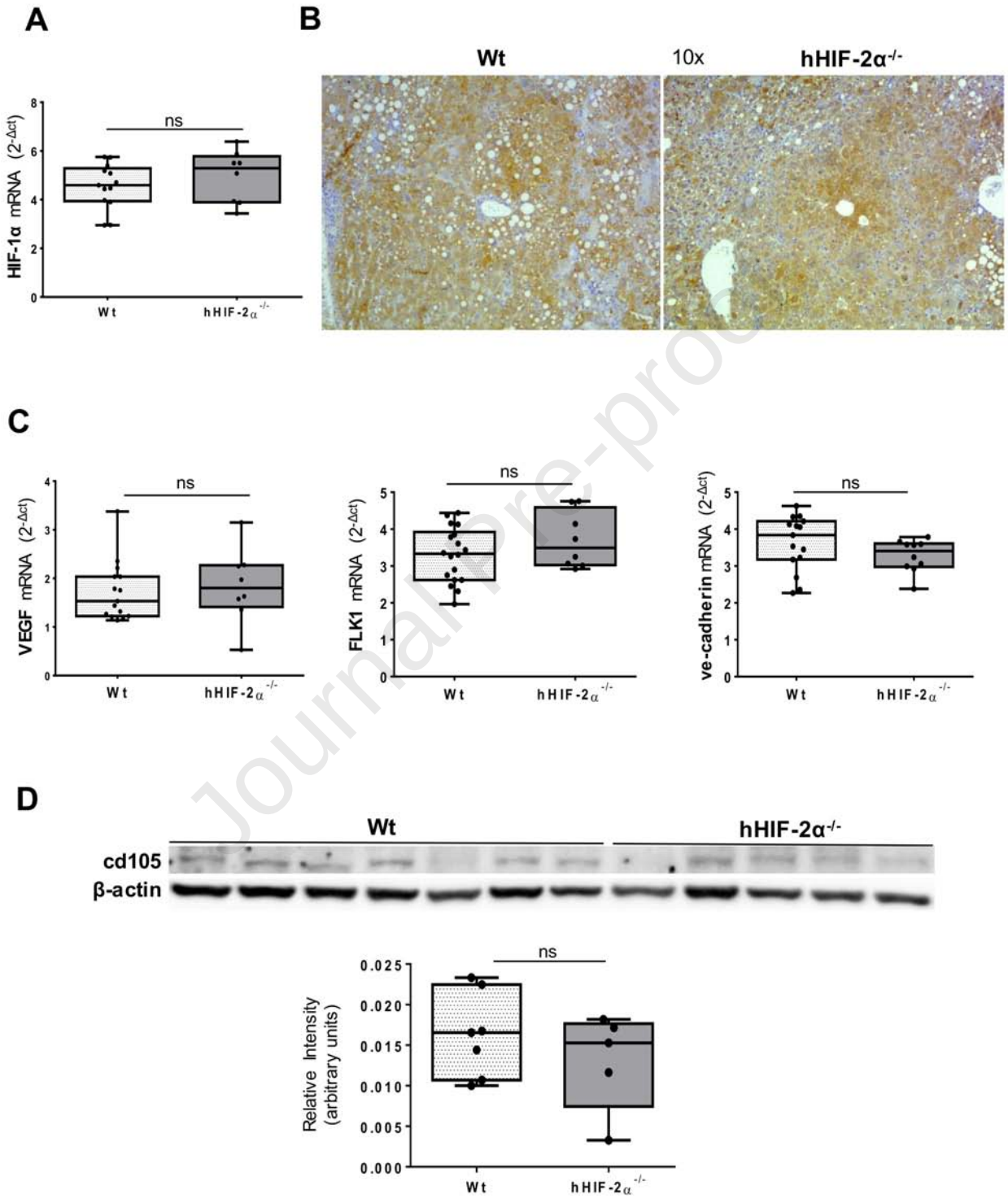

Figure 4

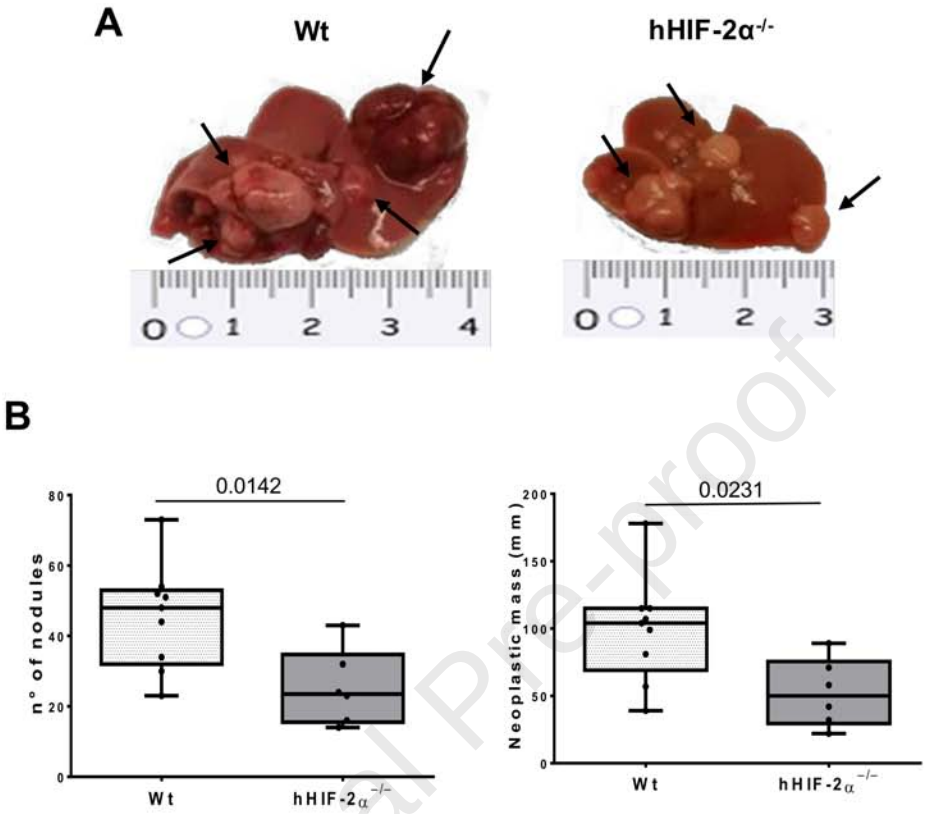

Figure 5

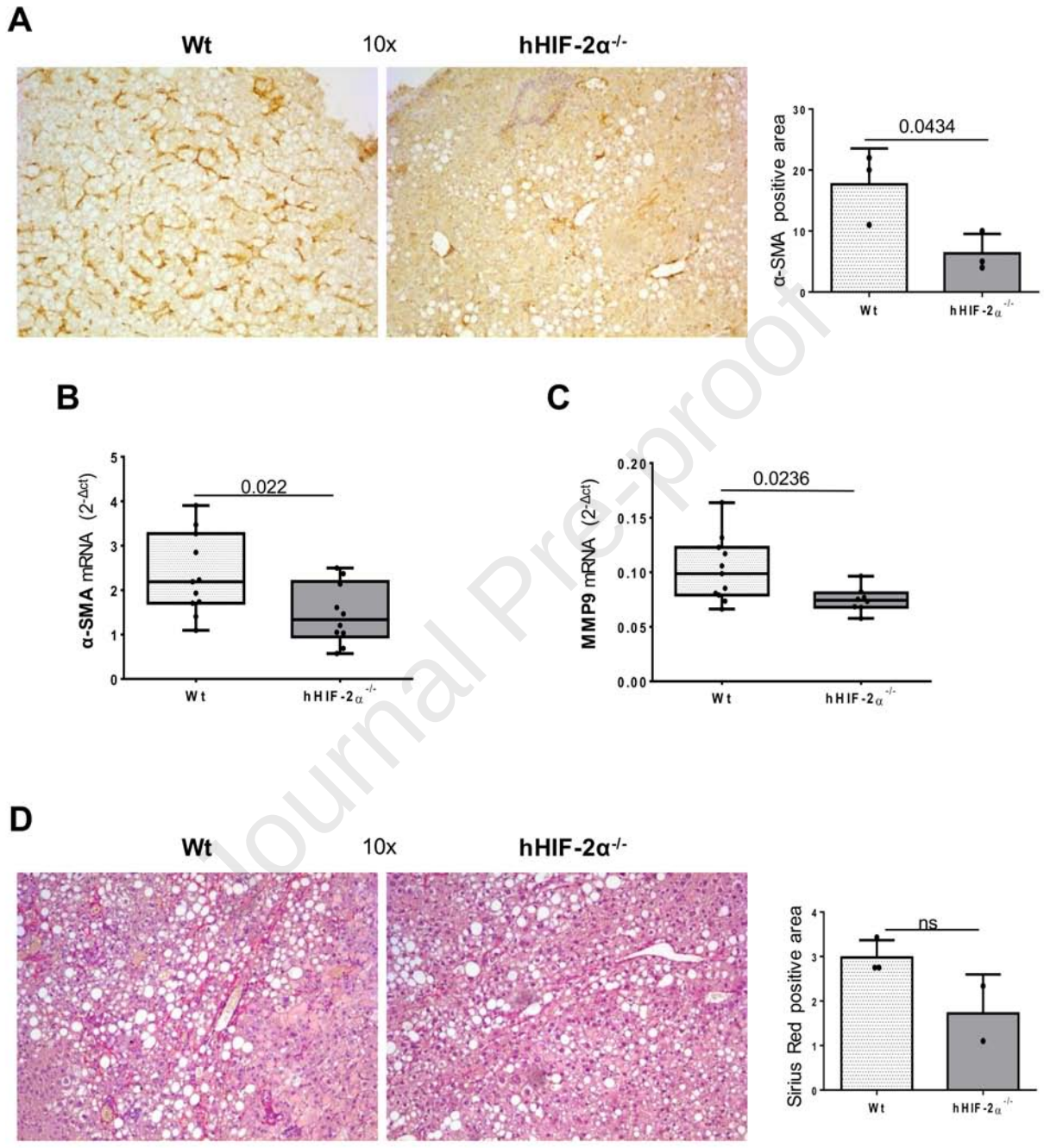

Figure 6

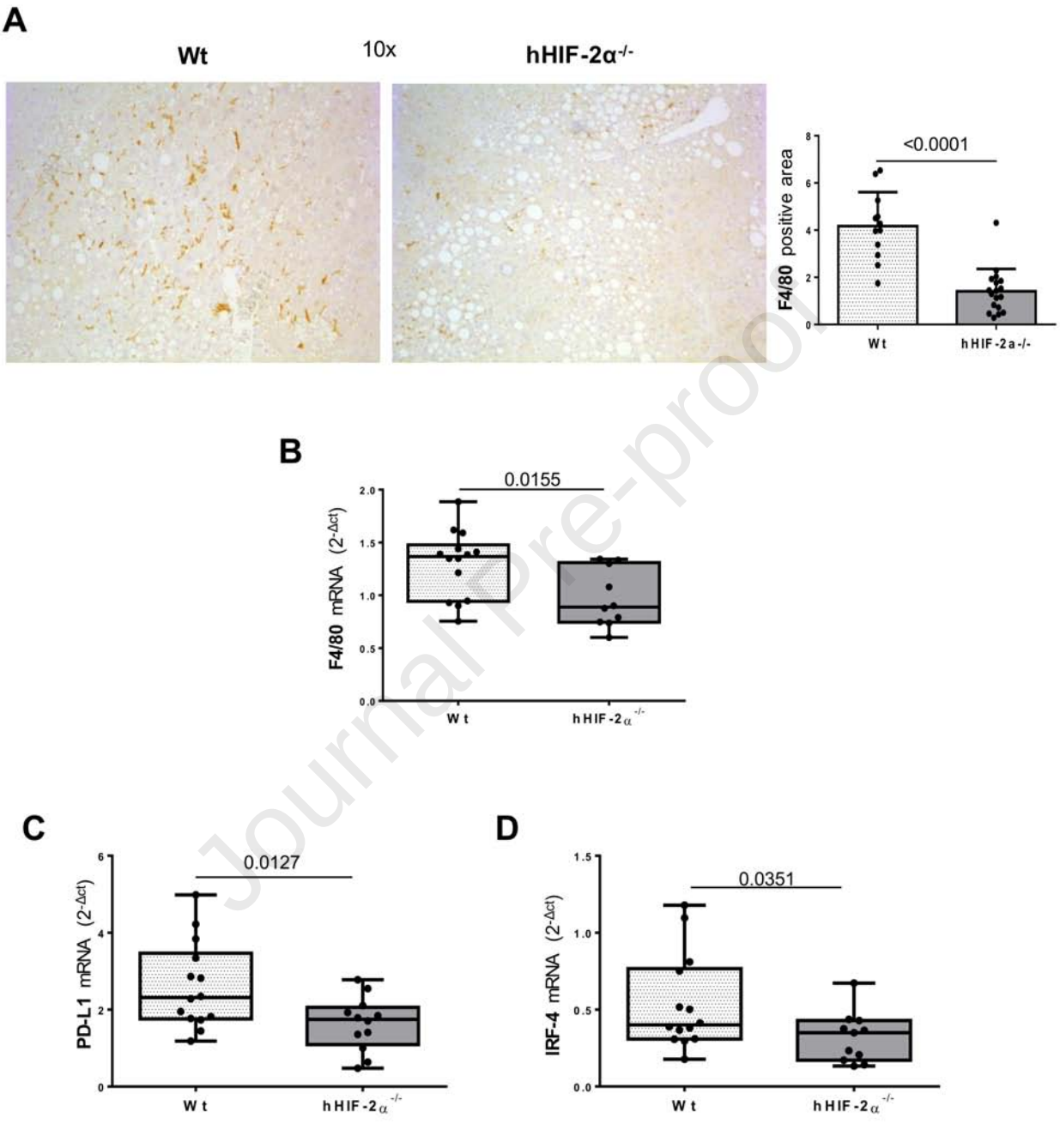

Figure 7

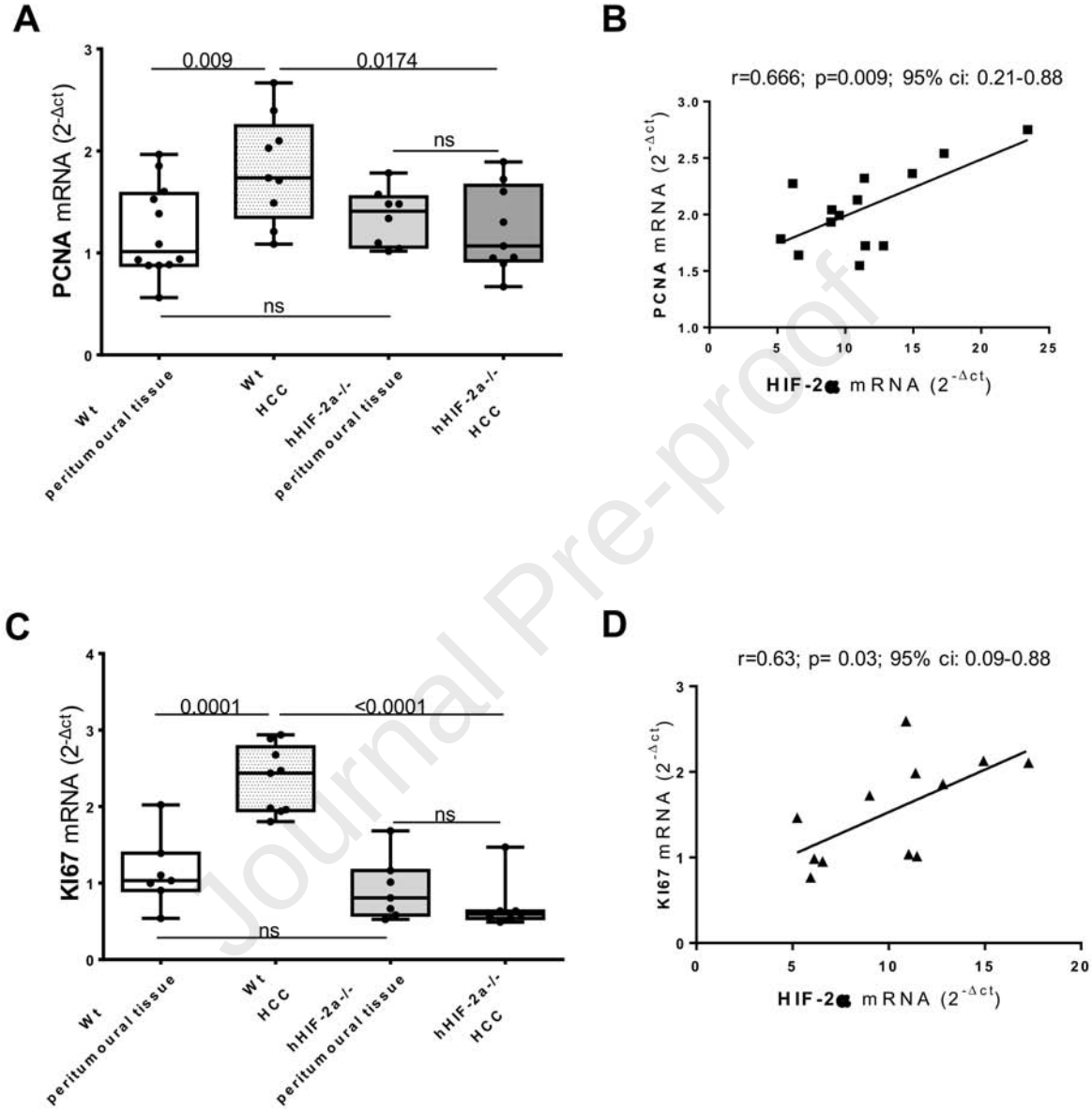

Figure 8

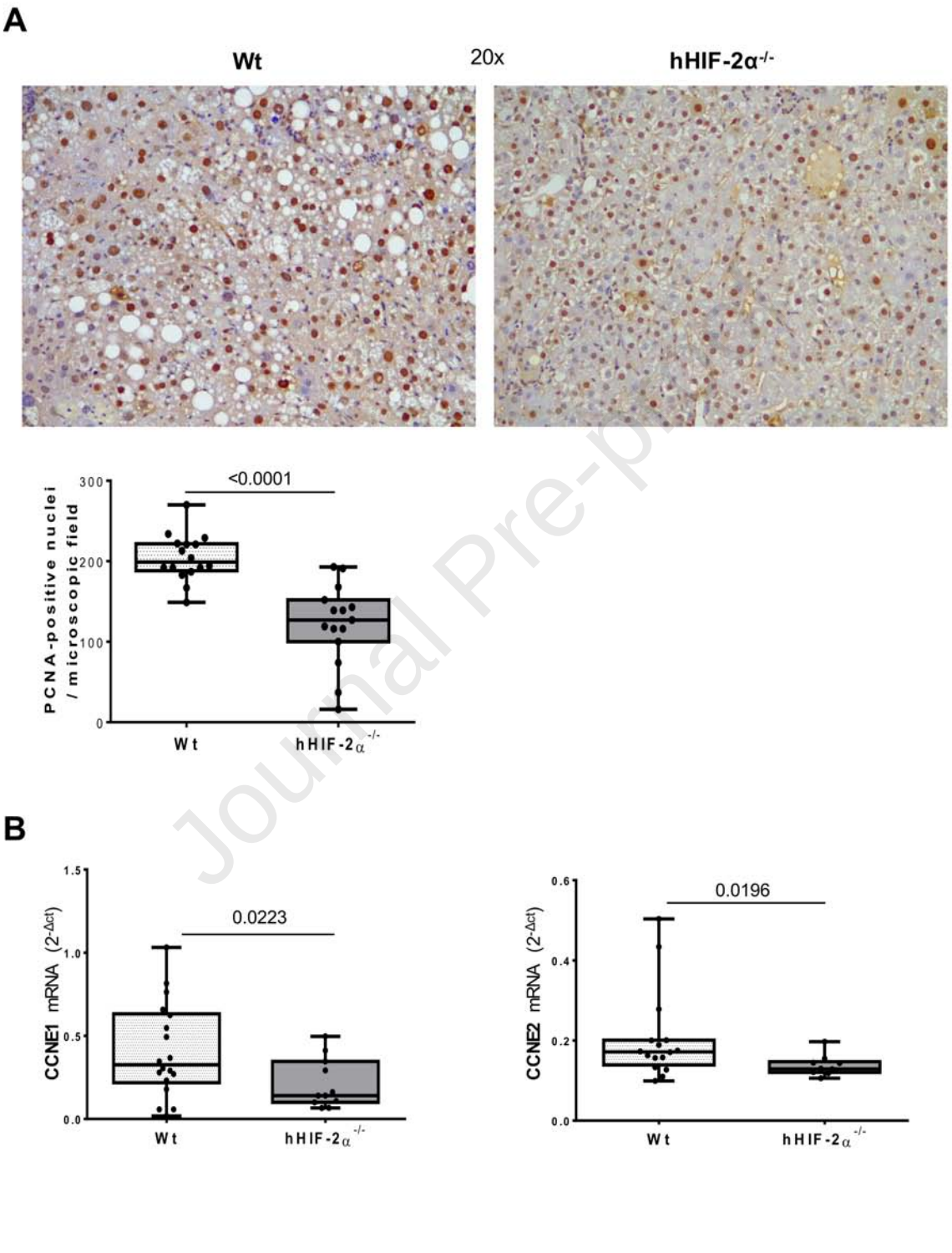

Figure 9

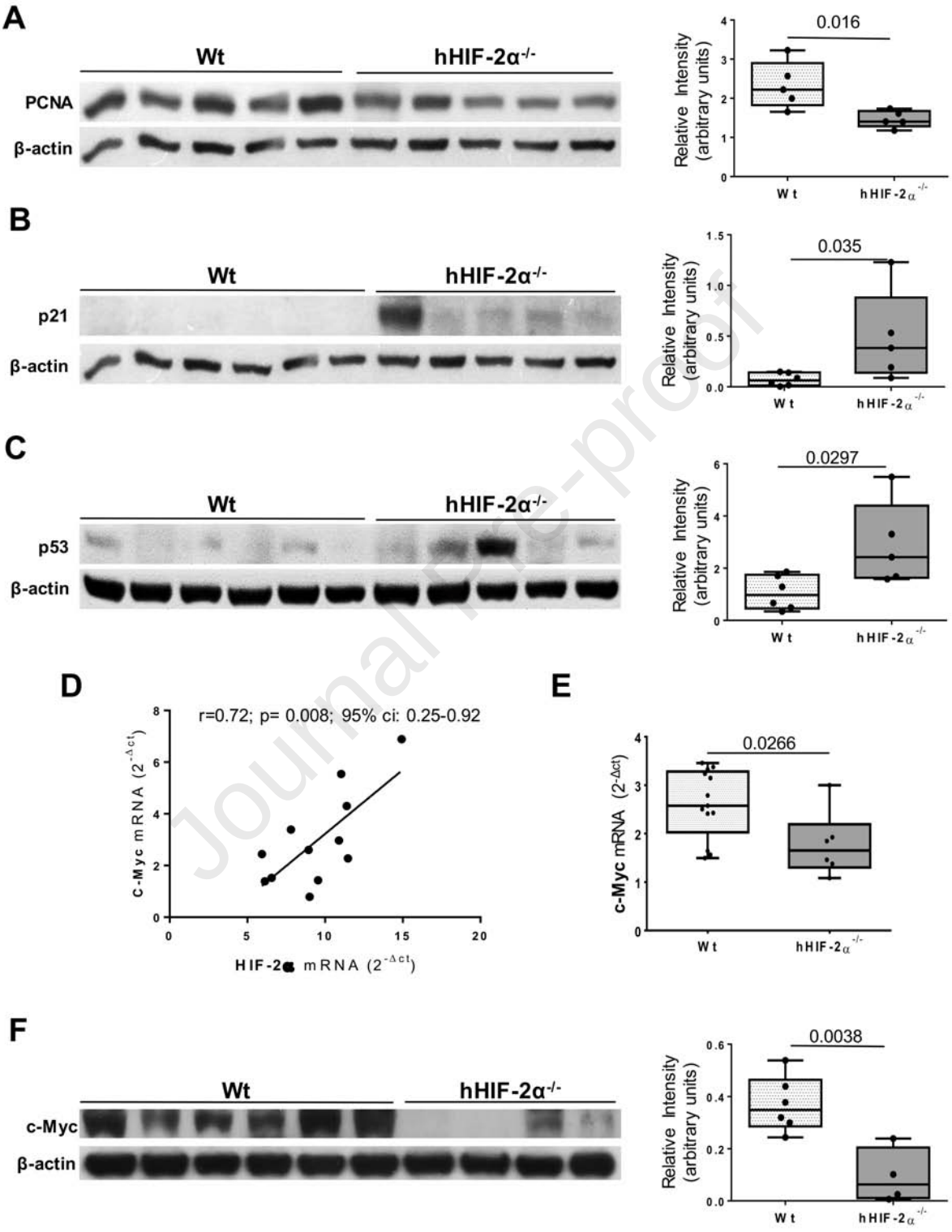

Figure 10

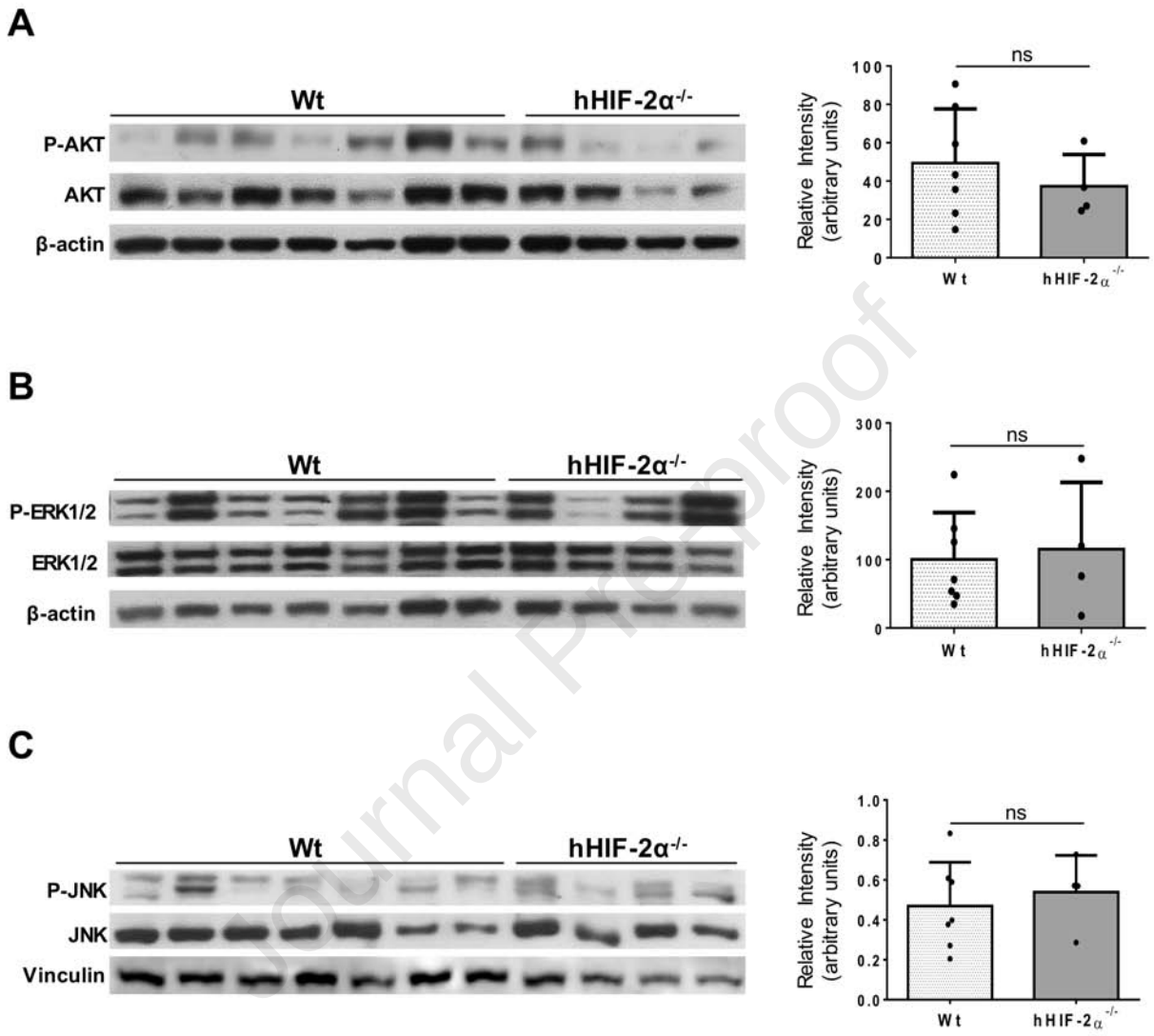

Figure 11

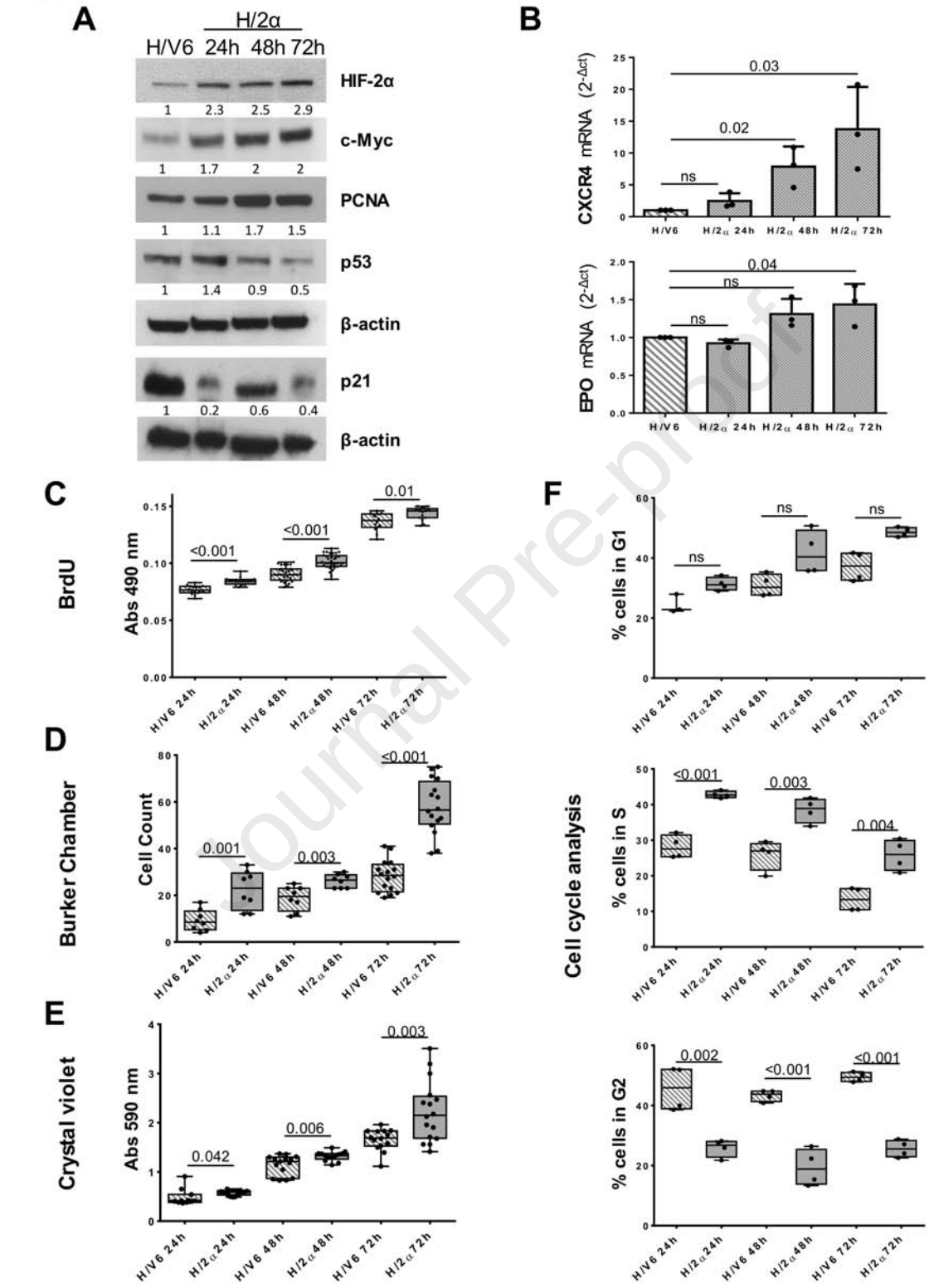

Figure 12

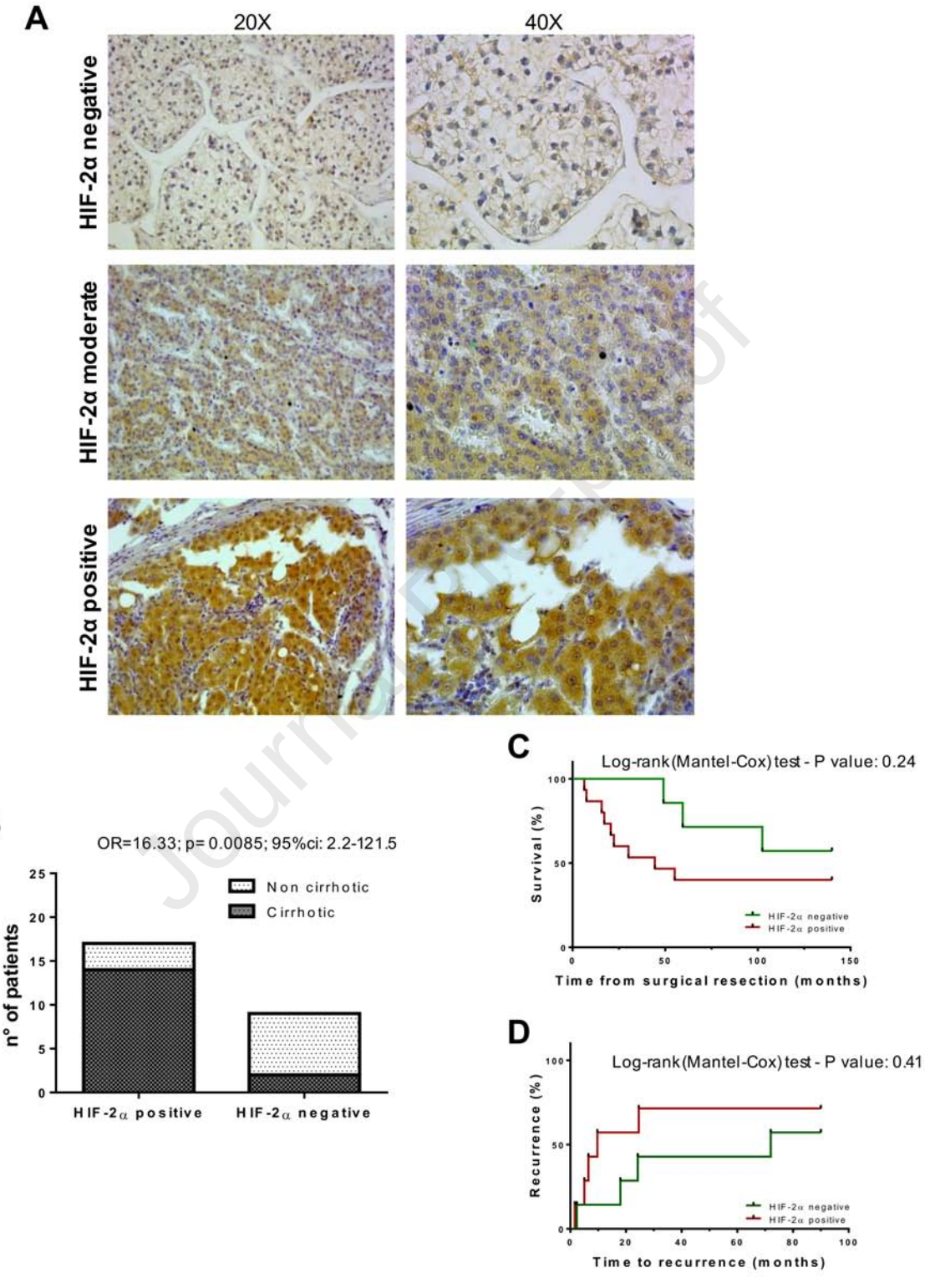

Figure 13

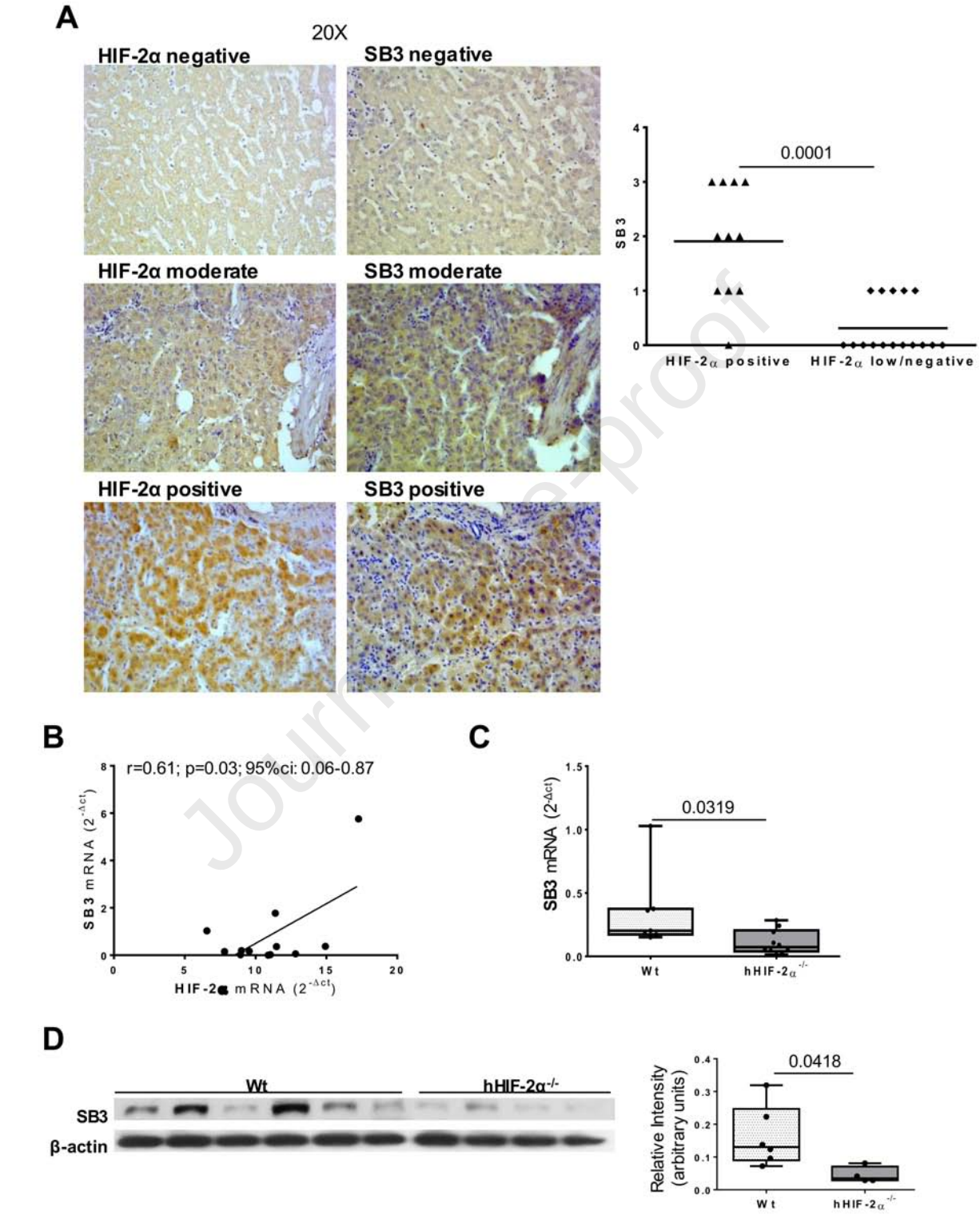

Figure 14